037298-1-T

Design and Evaluation of an 18" Cavity Backed Slot Spiral for UHF to L band Operation

Michael Nurnberger
John L. Volakis

USAF
AFMC, AFRL/IFKRD
26 Electronic Pky
Rome, NY 13441-4514

April 1999

37298-1-T = RL-2513

PROJECT INFORMATION

PROJECT TITLE: New Thin Slot Spiral Antenna for Multiband Communications on UAVs

REPORT TITLE: Design and Evaluation of an 18" Cavity Backed Slot Spiral for UHF to L band Operation

U-M REPORT No.: 037298-1-T

CONTRACT
START DATE: August 1998
END DATE: January 2000

DATE: April 1, 1999

SPONSOR: Donald Pflug/Steven Reichhart
Air Force Research Laboratory
Rome Research Office
AFRL/IFGC
525 Brooks Rd
Rome, NY 13441-4505
Phone: 315-330-4290 FAX: 315-330-7137
Pflugd@rl.af.mil

SPONSOR
CONTRACT No.: F30602-98-C-0233

U-M PRINCIPAL
INVESTIGATOR: John L. Volakis
EECS Dept.
University of Michigan
1301 Beal Ave
Ann Arbor, MI 48109-2122
Phone: (313) 764-0500 FAX: (313) 747-2106
volakis@umich.edu
http://www-personal.engin.umich.edu/~volakis/

CONTRIBUTORS
TO THIS REPORT: Michael W. Nurnberger and J.L. Volakis

Abstract

This report reviews the progress made in the first half of the overall effort towards the development of an electrically small, efficient, shallow, and extremely broadband (30 MHz to 2 GHz) slot spiral antenna. The state-of-the-art before the start of this effort was a six inch diameter slot spiral with a 5.5-inch diameter aperture having a gain of at least 4 dB_i from 800 MHz to 5 GHz, nearly hemispherical coverage, and low axial ratio [1]. New techniques have been developed since then to greatly extend the low frequency cutoff and overall bandwidth of the slot spiral antenna and are presented herewith. Also, results are presented from the measurement of an 18-inch diameter slot spiral designed to achieve a 40:1 bandwidth (100 MHz to greater than 4 GHz). Finally, plans for the second half of the effort that detail the development and testing of the final 36-inch square, 30 MHz to greater than 2 GHz slot spiral antenna are presented.

Contents

1 Overview and Project Goals

This report reviews the progress made in the first half of the overall effort toward the development of an electrically small, efficient, shallow slot spiral antenna. The state of the art before this effort was the six inch diameter slot spiral shown in Figures 1, 2, and 3, in Appendix D (top, bottom, and cavity configuration, respectively). This antenna has a 5.5-inch diameter radiating aperture with at least 4 dB_i of gain from 800 MHz to 5 GHz, nearly hemispherical pattern coverage, and low axial ratio [1].

In the first half of this effort, the frequency range of this antenna has been extended by a factor of eight ($\times 8$), from 800 MHz down to 100 MHz, yielding an overall antenna frequency coverage of 100 MHz to greater than 4 GHz with a total bandwidth of approximately 40:1. New miniaturization techniques have also been introduced and applied that permit this increase with just a factor of four ($\times 4$) increase in overall diameter, currently only 18 inches. Thus, a factor of two ($\times 2$) reduction in the overall size of the antenna has been achieved for an extremely broad operating frequency range while still maintaining good gain, pattern coverage, and polarization characteristics.

The ultimate goal of this effort is to construct an antenna with 100:1 bandwidth that operates from 30 MHz to 3 GHz while still fitting into a 36 $\times$ 36-inch square region. As originally discussed in the proposal, the reduction of the lowest operating frequency to 100 MHz can be extrapolated from the previous technology. Further reduction to 30 MHz without any size increase is significantly more risky. Nevertheless, the measurements so far show substantial promise that operation down to 30 MHz withing the aforementioned size limits can indeed be achieved. This entails a further factor of three ($\times 3$) increase in bandwidth.

Clearly, a factor of two ($\times 2$) increase in bandwidth can be obtained simply by scaling the antenna to fit into the larger square aperture. The final factor of one and one-half

($\times 1.5$) can be obtained by increasing the amount of miniaturization through increase inductive loading, as discussed below, possibly in concert with other miniaturization techniques. These include further loading of the transmission line with lumped element chip capacitors and the application of high-dielectric constant materials to the aperture and/or inside the cavity. The optimum combination of these techniques will be implemented in the final antenna.

2 Progress & Accomplishments

2.1 Introduction

Prior to this effort, the state-of-the-art slot spiral antenna consisted of a six inch diameter antenna that was approximately one-half inch thick. As mentioned above, it had at least 4 dB_i of gain from 800 to 4000 MHz for a operational bandwidth of approximately 5:1, nearly hemispherical pattern coverage, and good axial ratio.

In the nine months since the start of this effort, the bandwidth capability of the slot spiral has been increased by a factor of eight ($\times 8$) to 40:1, with a frequency response from 100 MHz to 4 GHz. A size reduction of a factor of two has also been introduced, decreasing the actual size of the antenna from its previous diameter of 36 inches to 18 inches in diameter. Four types of test articles were fabricated to validate these advances—normal (unloaded) and inductively loaded versions of a 6-inch diameter antenna, and normal (unloaded and inductively loaded versions of a 18-inch diameter antenna. Pattern and input impedance measurements were made on the 18-inch diameter antennas as reported in the review. Work is underway to improve the performance of the current 18-inch spiral, and a final design for the overall size-bandwidth requirements of a 30 MHz to 2 GHz antenna with an aperture that fits in a 36-inch square is under consideration.

These dramatic improvements in performance were made possible by the introduction of two new developments. A new transition and lumped element structure were developed and combined to provide a good termination for the slot arms down to DC, thereby enabling proper operation of the antenna at low frequencies. Various miniaturization techniques were applied as well to decrease the overall size of the antenna, including a novel method of frequency-independent inductive loading. Each of these techniques are discussed in more detail below.

2.2 Lumped Element Termination

The previous 6-inch diameter antenna mentioned above employed a resistive thick-film termination over the last half-turn of the radiating slot to attenuate reflections from the slot arm ends. However, this termination does not perform as well as desired at the lowest frequencies, and tends to prematurely attenuate the low-frequency energy prior to its radiation. Fabrication of the thick film termination was also complicated by the inconsistency of and lack of control over the resistivity of the film. Furthermore, because of shrinking physical dimensions and tighter tolerances, all these difficulties are exacerbated when the antenna is miniaturized.

By transitioning the radiating slotline to a twin-wire line, or co-planar strips (CPS) before the application of a termination, these and other difficulties associated with the construction of a high-quality, very broadband termination can be overcome. Once the transition is made to CPS, the fabrication of series elements is made possible, allowing new approaches to the termination problem. A broadband impedance transformer is used to perform this geometry change to ensure that very little energy is reflected.

The existance of series elements, which before were impossible due to the structure of slot line, allows the fabrication and use of matched attenuators to implement the ter-

mination. Lumped elements are used to develop attenuator blocks with predetermined impedance and attenuation, and these are cascaded to provide sufficient termination of the energy reflected from the slot arm ends. The advantages of these matched attenuators are their extreme low-frequency performance (all the way to DC) and their size. Sufficient attenuation, even at the lowest frequencies, can be provided in a space less than 2 inches long, as compared to the approximately 24 inch length required for a thick-film termination for the 18-inch diameter antenna mentioned above. This allows better aperture utilization, greater gain at lower frequencies, and better axial ratio across the entire operating frequency range. The lumped element termination is discussed in more depth in Appendix A, Sections A.7–A.9.

2.3 Inductive Loading for Aperture Miniaturization

At the lowest operating frequencies, the slot spiral radiates from its outermost region, where it is approximately one wavelength in circumference. Thus, to decrease its lowest operating frequency, standard practice is to increase the diameter of the antenna. The same effect, however, may be obtained by decreasing the guide wavelength along, or inside, the slot.

The most common way of doing this is to apply dielectric loading to the slotline (compare Figures 3 and 24), slowing down the wave by a factor of up to $0.5/\sqrt{\epsilon_r}$. However, this may cause undesirable modes in the cavity, and will increase both the cost and the weight of the antenna. An alternative method for reducing the guide wavelength is the application of series inductive loading along the slot. In essence, the edges of the slotline are lined with thousands of electrically short, short-circuited slot stubs, as shown in Figure 19, which combine to increase the inductance per unit length of the slot, thus slowing the wave down. This method has the added advantage of being completely planar, as it shares the same metallization layer the slotline is etched in. In the case of the current slot spiral, a reduction

by a factor of two ($\times 2$) was achieved in the guide wavelength in the slotline by increasing the series inductance per unit length by a factor of four ($\times 4$). This translates directly into an overall antenna size reduction of a factor of two ($\times 2$). The design and implementation of the inductive loading is discussed in more detail in Appendix A, Section A.6.

2.4 Antenna Prototype Description

To validate these new techniques and verify the resulting low-frequency extension, several antenna prototypes were designed and fabricated. These were divided into two sets. A first set of six inch diameter antennas were built to compare and validate the performance of the new termination and loading techniques against the previous state-of-the-art slot spiral. The antennas in the second set were 18 inches in diameter, and designed to demonstrate the feasibility of the more broadband aperture. In each of these sets—the 6-inch diameter set and the 18-inch diameter set—two types of antennas were fabricated. One type was designed to serve as the experimental control, and contained no inductive loading. The other type was inductively loaded, allowing a measure of the effectivness of the inductive loading to be obtained. At least two antennas of each type, in each set, were fabricated to allow for some experimentation and possible accidental loss or destruction.

2.5 Performance Goals

As determined by its outer circumference, the 6-inch diameter unloaded antenna should have positive gain and low axial ratio down to approximately 750–800 MHz. Similarly, the 18-inch diameter unloaded antenna should have positive gain down to approximately 250 MHz—an increase in diameter by a factor of three implies a decrease in operating frequency by the same factor of three. As was discussed above, for both cases, the inductive loading was designed to decrease the guided wavelength in the slotline by a factor of

two. Therefore, the inductively loaded version of these two antennas should operate down to half the lowest operating frequencies of their counterparts—375 MHz and 125 MHz, respectively.

2.6 Measurements

2.6.1 Introduction

Of the antennas discussed above that were designed and fabricated, only the 18-inch diameter versions have been tested so far. Pattern measurements were made at Rome Labs, along with preliminary input impedance tests. Some measurements of the previous state-of-the-art slot spiral were made as sanity checks, but time did not allow measurement of the new 6-inch diameter antennas for comparison.

The next section gives a detailed description of the measurements made at Rome Labs. Discussion of the measured data, along with graphs of the resulting gain, axial ratio, and pattern information follow. Actual patterns are shown in Appendix C.

2.6.2 Description of Measurements at Rome Labs, February 8–13, 1999

Measurements Performed:

1. Chamber qualifications to verify polarization performance down to 100 MHz. Measured by locking both transmit and receive horns together and spinning them simultaneously. Any variation in the received power must be due to the stationary portions of the system—chamber, rotary joints, etc.

2. Source Horn Validation:

   EMCO 3106 Dual-Ridge Broadband Horn

   - E- & H-plane cuts from 100 MHz to 2 GHz, 100 MHz steps
   - Measurement goal was to determine the polarization purity of the horns for the above frequencies.

   EMCO 3106 & 3115 Dual-Ridge Broadband Horns

- E- & H-plane cuts at 1000, 1500, 2000 MHz
- Measurement goal was to determine the polarization purity of the horns for the above frequencies.

3. Previous spiral antenna: SPI6.4

   - Spinning linear azimuth cuts: $\pm 120°$, various frequencies between 1 and 4 GHz
   - Served to verify measurement system—a crude but useful sanity check, particularly of the AUT test setup. Patterns from these measurements were compared with patterns from previous measurements of the same antenna performed at NASA Langley [2, 3].

4. Unloaded 18" spiral: SPI9.2

   - Spinning linear azimuth cuts: $\pm 120°$
   - Several AUT orientations (every 90°)

     Equivalent to E- & H-plane cuts on linear-polarized antenna
     Also to differentiate between antenna and chamber effects
   - Frequencies:

     100 MHz, 150 MHz
     200 – 2500 MHz, 100 MHz steps
     2750, 3000 MHz

5. Loaded 18" spiral: SPI8.2

   - Spinning linear azimuth cuts: $\pm 120°$
   - Several AUT orientations (every 90°)

     Equivalent to E- & H-plane cuts on linear linear-polarized antenna
     Also to differentiate between antenna and chamber effects
   - Frequencies:

     100 MHz, 150 MHz
     200 – 2500 MHz, 100 MHz steps
     2750, 3000 MHz

6. Other measurements besides those outlined above for SPI8.2 and SPI9.2 were performed for debugging purposes. Many of the measurements for SPI9.2 were performed later by John Streeter and Dan Warren, of Rome Research Corporation and of Rome Laboratories, respectively.

2.6.3 Test Results & Conclusions

As mentioned in the previous section, radiation patterns of both the unloaded and loaded 18-inch diameter spirals where measured over an azimuth angular span of $\pm 120^{\circ}$ using a spinning linear source. Figure 4 gives a schematic description of the measurement setup in the anechoic chamber. The full set of patterns for both the unloaded and loaded 18-inch diameter antennas is included in Appendix C. From these patterns, boresight gain and axial ratio were extracted, and are plotted with respect to frequency in Figures 5 and 6.

Generally, the radiation pattern of a spiral antenna is expected to remain fairly similar over the operational frequency range of the antenna. This implies that both the gain and axial ratio curves should also be relatively flat and uninteresting. A quick scan of the patterns in Appendix C, and of the gain and axial ratio plots in Figures 5 and 6, however, shows that the current performance of the slot spiral antenna is anything but uninteresting. Even the unloaded spiral, which very nearly follows all the standard guidelines for frequency-independent structures [4], has very inconsistent performance. Briefly, the following general observations can be made:

1. Both axial ratio and gain are oscillatory in nature.

2. Pattern shape is highly inconsistent except at the lowest frequencies.

3. Low frequency gain is very poor compared to the expected values mentioned above.

These difficulties are the results of several problems, both with the antennas and with their surroundings. Each of the three general observations is dealt with separately below.

Oscillatory Axial Ratio

The axial ratio of a spiral antenna provides a great deal of information about its inner workings. Low axial ratios imply nearly circular polarized radiation, which is the natural

mode radiated by the slot spiral. They are the best indication that the spiral is operating in a frequency-independent manner. Higher axial ratios imply contamination of this circular mode by other radiation, most often a result of poor arm termination or interactions with the antenna's surroundings *i*.e. measurement setup. Thus, measurement of the axial ratio provides a direct indication of the performance of the termination, and when combined with other measurements can also indicate pattern distortion from the measurement setup. With printed (wire) spirals, because of their more narrow radiation pattern, it is usual to neglect the surroundings, and concentrate strictly on the antenna. However, as will be discussed in more detail below, this luxury is not available with the slot spiral antenna.

Leaving the issue of effects due to the antenna's surroundings until later, the other major source of increased axial ratio is reflections somewhere along the radiating arm of the spiral. This is often the result of an insufficient arm termination, or a fabrication error that results in a distortion of the arm and a change in impedance. Any energy that reflects from one of these discontinuities and reradiates distorts the basic circular polarization of the antenna. It is important to note that this distortion is frequency dependent as well, as the relative phase between the initial radiation and the radiation from the reflected energy is a function of distance, which is in turn a function of frequency.

After careful inspection, several sources of reflections were found in both the unloaded and loaded antennas. It was found that the terminations on both antennas were not as well matched as originally thought, and require the addition of another matching resistor. This in itself is sufficient to explain the poor axial ratio of the unloaded antenna at low frequencies. The loaded antenna contains two other sources of reflection as well, both having to do with the integration of the series inductive loading shown in Figures 11 and 19. Near the center of the antenna, the inductive loading is introduced too rapidly, resulting in a reflection at that point. That is, the length of the shorted slot stubs initially increases too rapidly, adding inductance too quickly and creating an overly-rapid change in impedance which causes a

reflection. At the transition from the inductive loading to the resistive termination, while the impedances are appropriately matched, the change in the field structure is too great, also causing a very large reflection just before the termination. Thus, while terminated, it still behaves almost as an unterminated spiral.

Clearly, having identified the sources of these reflections, steps can be taken to remove them. The resistive termination has already been corrected by the addition of a few more matching resistors. The discontinuities at the start and end of the inductive loading section will be removed from the current design by using copper tape to adjust the stub lengths, thus more properly tapering the transitions and ensuring a better impedance match. Designs of future antennas will take these modifications into account and minimize the disturbances at these locations.

Poor Pattern Shape and Oscillatory Gain

The radiation pattern of a spiral antenna should remain consistent in size and shape over its entire bandwidth, baring external frequency-dependent disturbances. Comparison of the radiation patterns of the unloaded spiral measured at 700, 800, and 900 MHz give a good example of this situation. At 700 and 900 MHz, the spinning linear radiation patterns are reasonably acceptable, and the axial ratio is relatively consistent across the entire hemisphere. At 800 MHz, however, there is greatly increased axial ratio both at boresight and towards the horizon, and large, deep nulls at approximately $45°$ from boresite. Narrowband anomalies of this sort in the middle of the operating frequency range are not expected for a 20:1 bandwidth spiral antenna. They therefore must be caused by some external interaction.

The radiation pattern of a slot spiral also should not "tuck in" so dramatically near the horizon, at $\pm 90°$. Both of these effects can be traced to the same source—diffraction from the edges of the ground plane that the slot spiral is mounted on. At the lowest frequencies, little effect is seen, because the ground plane is relatively small compared to the operating

wavelength. As the frequency increases, however, the effects become more pronounced, as can be seen from the patterns in Appendix C. The nulling in the radiation pattern and the rapidly varying axial ratio are both a result of the amplitude and polarization sensitivity of the diffracted fields—they are in general linearly polarized, with magnitude and orientation a function of both location around the circumference of the ground plane and of frequency. The oscillations in the gain that were mentioned in passing above are also tracable in part to these effects.

The ground plane diffraction problem has plagued the slot spiral since its conception. Particularly at low frequencies, it is difficult to treat this problem with the standard techniques of rolled or absorber/R-card loaded edges due to the very large required dimensions. Recent advancements in computational electromagnetics now offer the possibility of numerically removing these effects, however, and are being investigated currently.

Poor Low Frequency Gain

The last general observation made was that the gain of both the unloaded and loaded antennas drops off much before the expected low-frequency cutoff of the antenna—nearly a factor of two for the unloaded spiral, and a factor of three to four for the loaded spiral. Past experience has shown that this is generally a result of placing the reflecting cavity too close to the radiating slots. If the conducting cavity back is too close to the slotline, it interacts with the fields in the slotline, both before and during radiation. Prior to radiation, this interaction changes the field structure of the propagating mode in the slotline, greatly increasing its loss. During radiation, the conducting plane shorts some of the electric field in the slot, thereby reducing the amplitude of the fictitious magnetic currents that radiate. An example of this effect in shown in Figure 7, where an increase in low-frequency gain of approximately 4-5 dB is obtained by doubling the separation between the slot antenna and the reflecting cavity.

Deeper cavities have already been fabricated for both the loaded and unloaded antennas, and are ready to be installed after the modifications to the terminations are validated.

3 Up-to-Date Review of Current Status

As was mentioned before, four antenna prototypes were designed and fabricated—unloaded and loaded 6-inch diameter antennas, and unloaded and loaded 18-inch diameter antennas. The patterns and input impedance of the 18-inch diameter antennas were measured at the Rome Labs facility. These larger antennas incorporated both the new lumped element match attenuator resistive slot arm terminations and the series inductive loading scheme with the goal of achieving a 100 MHz to 4 GHz, 40:1 operational bandwidth antenna. Due to certain design flaws, the entire bandwidth was not achieved. As discussed above, these flaws have been isolated and are in the process of being repaired. The 18-inch diameter antennas will be ready to be tested again by the end of May.

4 Current and Future Plans

To achieve the goals discussed above, namely a 100:1 bandwidth antenna that operates from 30 MHz up to 3 GHz and still fits into a 36 $\times$ 36 inch square, the following steps will be taken in the second half of this effort:

1. Finish repairs to the lumped element resistive termination.

2. Finish modifications to the inductive loading to minimize the discontinuities.

3. Scale the antenna geometry by a factor of two ($\times 2$) to most efficiently fill the 36-inch square.

4. Further investigate and apply the most promising combination of loading techniques (inductive and dielectric) to achieve the most reduction in size for the least reduction in overall gain and pattern performance.

5. Investigate alternative cavity configurations to ensure the most broadband and high gain solution possible while minimizing overall cavity depth.

6. Further develop the accuracy of the new lumped element terminations to ensure better performance over the entire frequency range.

7. Develop better transitions to and from the inductive loading section to minimize reflections and decrease axial ratio.

8. Fabricate and measure at least one and probably two more models to verify antenna performance.

9. Develop a numerical method of removing the ground plane diffraction effects to more accurately measure the antenna's true performance.

10. Create CAD models and fabricate the final 36-inch antenna aperture.

11. Perform antenna simulations on C-130 and Global Hawk platforms.

5 Conclusions

In the first half of this effort the performance of the state-of-the-art slot spiral has been dramatically enhanced. The operational bandwidth was increased from 5:1 to nearly 40:1, and the low-frequency limit of the antenna was decreased by nearly a factor of eight ($\times 8$) while the maximum dimension of the antenna was only increased by a factor of four ($\times 4$).

Several performance difficulties were encountered, but their sources have been identified and are being resolved. Modified antennas will be ready for re-measurement by the end of May.

A further increase in low-frequency extension by a factor of three is necessary to achieve operation down to 30 MHz. Several methods wil be pursued towards this goal, among them a factor of two ($\times 2$) increase in size to a 36-inch square. The optimal combination of dielectric loading and increased inductive loading will also be incorporated to ensure the best gain, axial ratio, and pattern performance possible.

References

[1] M. W. Nurnberger, T. Özdemir, J. L. Volakis, "A Planar Slot Spiral for Multifunction Communications Apertures," 1998 AP-S International Symposium and URSI Radio Science Meeting, Atlanta, GA, June, 1998.

[2] M. W. Nurnberger, J. L. Volakis, D.T. Fralick, F.B. Beck, "A Planar Slot Spiral for Conformal Vehicle Applications," 18th Meeting and Symposium of Antenna Measurement Techniques Association, Seattle, WA, September, 1996.

[3] M. W. Nurnberger and J. L. Volakis, "A Planar Slot Spiral for Mobile Communications," 19th Meeting and Symposium of Antenna Measurement Techniques Association, Boston, MA, November, 1997.

[4] V. H. Rumsey, *Frequency Independent Antennas*, Academic Press, 1966.

[5] J. S. Izadian, S. M. Izadian, *Microwave Transition Design*, Artech House, 1988.

[6] N. Marchand, "Transmission Line Conversion Transformers", Electronics, Vol. 17, pp. 142–145, December, 1944.

[7] R. Bawer, J. J. Wolfe, "A Printed Circuit Balun for Use with Spiral Antennas," IRE Trans. Microwave Theory Tech., Vol. MTT-8, pp. 319–325, May, 1960

[8] G. Oltman, "The Compensated Balun," IEEE Trans. Microwave Theory Tech., Vol. MTT-14, pp. 112–119, March, 1966.

[9] V. Trifunović, B. Jokanović, "Review of Printed Marchand and Double Y Baluns: Characteristics and Application," IEEE Trans. Microwave Theory Tech., Vol. MTT-42, pp. 1454–1462, August, 1994.

[10] J. D. Dyson, "The Equiangular Spiral Antenna," IRE Trans. Antennas Propagat., Vol. AP-7, pp. 181–187, April, 1959.

[11] M. W. Nurnberger, J. L. Volakis, "A New Planar Feed for Slot Spiral Antennas," IEEE Trans. Antennas Propagat., Vol. AP-44, pp. 130-131, Jan 1996.

[12] R. W. Klopfenstein, "A Transmission Line Taper of Improved Design," Proc. IRE, Vol. 44, pp. 31–35, January, 1956.

[13] S. B. Cohn, "Slot Line on a Dielectric Substrate," IEEE Trans. Microwave Theory Tech., Vol. MTT-17, pp. 768–778, October, 1969.

[14] E. A. Mariani, C. P. Heinzman, J. P. Agrios, S. B. Cohn, "Slot Line Characteristics," IEEE Trans. Microwave Theory Tech., Vol. MTT-17, pp. 1091–1096, December, 1969.

[15] G. H. Robinson, J. L. Allen, "Slot Line Application to Miniature Ferrite Devices," IEEE Trans. Microwave Theory Tech., Vol. MTT-17, pp. 1097–1101, December, 1969.

[16] J. B. Knorr, "Slot-Line Transitions," IEEE Trans. Microwave Theory Tech., Vol. MTT-22, pp. 548–554, May, 1974.

[17] W. L. Curtis, "Spiral Antennas," IRE Trans. Antennas Propagat., Vol. AP-8, pp. 298–306, May, 1960.

[18] J. A. Kaiser, "The Archimedean Two-Wire Spiral Antenna," IRE Trans. Antennas Propagat., Vol. AP-8, pp. 312–323, May, 1960.

[19] M. S. Wheeler, "On the Radiation from Several Regions in Spiral Antennas," IRE Trans. Antennas Propagat., Vol. AP-9, pp. 100–102, January, 1961.

[20] R. G. Corzine, J. A. Mosko, *"Four-Arm Spiral Antennas,"* Artech House, 1990.

Appendices

A Parts and Workings of the Current Slot Spiral Antenna

A.1 Introduction

The current slot spiral antenna can be divided into eleven individual but tightly coupled pieces or subsystems. The following sections discuss each one, giving pertinent background information and describing the implementation of each portion. Figures 8 and 9 show respectively the top and bottom views of the unloaded slot spiral that was used as the control, and Figures 10 and 11 show respectively the top and bottom views of the inductively loaded slot spiral Figure 12 gives a cut-away view of a slot spiral antenna with its accompanying shallow reflecting cavity.

A.2 Coaxial-to-Microstrip Line Transition

It is necessary to provide a means to connect the antenna to external devices, in particular for testing, prototype use, etc. Independent of the actual technique used, the means of connection must guarantee that it does not compromise the performance of the antenna in terms of bandwidth, VSWR, and leakage or radiation. While these issues are not normally of concern, they must be considered here because of the extremely broadband nature of the antenna.

Direct conversion from the microstrip infinite balun to coaxial cable was chosen as the best compromise between performance and ease of implementation. The location of the coaxial-microstrip transition in the current antennas can be seen in Figures 8–11. Several techniques have been developed for connecting coaxial and microstrip lines [5]. Initially, the right-angle transition shown in Figure 13 was used and performed adequately. However, due to mechanical strength and fabrication issues, a cheaper, more low-profile transition was implemented, and is shown in Figure 14. It avoids use of a connector entirely, greatly

reducing the expense of the antenna. It also more efficiently uses existing real estate and allows for more compact mounting, and minimizes any interactions of the cable with the radiated field. Its broadband performance is also quite impressive.

A.3 Microstrip Infinite Balun

The slot spiral antenna is a balanced antenna. As discussed in the last subsection, the most common method of connection to a low-power antenna is by coaxial transmission line, which is generally considered to be unbalanced. Thus, as with dipole and other balanced antennas, a balun (contraction for "balanced-to-unbalanced") is required to eliminate leakage currents which cause feedline radiation and aperture current disturbances.

The literature is replete with various examples of balun structures. Because of the extreme bandwidth of the slot spiral antenna, typical bandpass baluns of the Marchand type [6, 7, 8], which use resonant stubs, are inadequate. The so-called "double-Y" baluns are all-pass structures, and claim extremely wide-band performance if certain construction techniques are used [9]. However, the types of transmission line and dimensions used by Trifunovic, *et al.* to achieve this performance preclude planar implementation into the slot spiral antenna. The "infinite balun" first discussed by Dyson [10] is the only balun structure in the literature with bandwidth performance that automatically scales with the antenna, regardless of bandwidth. That is, it works equally well in a 10:1, a 30:1, or even a 100:1 bandwidth implementation.

Dyson realized his "infinite balun" by soldering the outer conductor of the coaxial feed line along the center of one of the arms of the antenna. However, the necessary dimensions, complexity, and expense involved in implementing Dyson's "infinite balun" in the slot spiral antenna for other than research purposes are prohibitive. To greatly simplify construction and reduce expenses, a similar "infinite balun" structure is realized using pla-

MISSING
PAGE

to-slotline transition. These finite-length, low-loss lines are the major source of the frequency-dependence that limited the attempts mentioned above.

- Elimination of open-circuit terminations for matching. Aside from radiation directly from the slotline, the slotline open-circuit in the transition of Figure 16 and the microstrip open-circuit in the transition of Figure 17 are responsible for the bulk of the observed radiation.

- Every port is matched over a very wide frequency range.

- The right-angle construction and symmetric configuration are an ideal solution for integration into the center region of the slot spiral antenna.

Many other broadband microstrip-to-slotline transitions have been developed in the last 30 years. However, most of them still include several elements that have significant frequency-dependence, if not actual resonant behavior in the operating frequency range, and also require a significant amount of real estate. Because of the very broadband performance achieved by the current implementation of the symmetric microstrip-to-slotline transition and its nearly ideal geometric layout, it seems to be the best transition for use with the slot spiral antenna.

A.5 Slotline

The radiating elements of the slot spiral antenna consist of two narrow slots etched in a spiral shape in an otherwise conducting surface. The overall layout is most easily understood from Figure 2 or 9, where the two slots are seen winding out from the center of the antenna, and from the cross-section in Figure 12. The two slots are connected together at the spiral's center, and together form the slot portion of the microstrip-to-slotline transition discussed above and shown in Figure 18.

The underlying geometry used in the earliest antennas was an archimedean spiral, defined by the equation

$$r = a\theta + b,$$

where

- r is the radial distance from the origin (mils),
- a is the spiral growth rate (mils/radian),
- θ is the angular position (radians), and
- b is the initial radial offset from the origin (mils).

The original 6-inch diameter spiral [1] with a gain of at least 4 dB from 800 MHz to 5 GHz (6.25:1 bandwidth) was designed with the following parameters: $a = 110.9$ mils/rad, $\theta = [-8\pi : 8\pi]$, and $b = 0$.

The current spiral antenna has a bandwidth of at least 30:1, with frequency coverage extending from about 100 MHz to at least 3 GHz. This is nearly five time more broadband than the 6-inch spiral discussed above. As expected, however, with this increased bandwidth comes increased losses, particularly in the microstrip balun at the higher frequencies. To reduce these losses, the current antenna uses a combination of both archimedean and exponential spirals. An archimedean spiral is used in the center of the antenna to allow proper tolerances and spacings to be maintained where the feed is accomplished, and where the high frequency energy is radiated. The rest of the antenna is made from exponential spirals of the form

$$r = b\, e^{a\theta}$$

with parameters similar to the archimedean spiral except for b, which becomes a scale factor. The exponential spirals allow conversion to a more rapid growth rate spiral, which reduces the number of turns necessary to cover a given frequency range. This in turns

reduces the length of both the spiral arms and the microstrip "infinite balun", dramatically reducing losses. Moreover, use of the exponential spiral form makes room for the inductive loading techniques discussed next by spacing the slots farther apart.

A.6 Inductive Loading

The basic theory of operation for a spiral antenna of either the printed or slot variety states that most of the radiation occurs from the annular region of the antenna that is approximately one guide wavelength in circumference [10, 17, 18, 19]. Most spiral antennas are built on thin, low-dielectric constant substrates, and have guide wavelengths that are on the order of 85–90% of the wavelength in free space. Thus, to radiate efficiently at a given frequency f, the antenna must have a diameter D of at least

$$D \gtrsim \frac{\lambda_g}{\pi} = \frac{v_p}{\pi f} = \frac{c}{\pi f \sqrt{\epsilon_{eff}}}$$

where

- λ_g is the guide wavelength in the slot,
- v_p is the velocity of propagation in the slot,
- ϵ_{eff} is the effective dielectric constant seen by the wave traveling in the slot, and
- c is the speed of light in a vacuum.

As operational frequency requirements drop below 500 MHz, the diameter given above gets large very quickly. At 500 MHz, $D \gtrsim 6.5$ inches. At 100 MHz, $D \gtrsim 32$ inches. Finally, at 30 MHz, $D \gtrsim 107$ inches, or nearly 9 feet in diameter. Clearly, these sizes are unsatisfactory for any sort of normal application. Thus, for operational frequencies in this range, some sort of miniaturization is required to reduce these sizes to something more manageable.

There are many miniaturization techniques often applied to antennas. The most common of these involve the use of higher dielectric constant substrate materials and the application of high dielectric constant materials to the antenna aperture. However, these techniques only work well with resonant antennas, where the fields are confined to a resonant cavity or other small region. Spiral antennas are not resonant antennas, instead belonging to the traveling wave antennas class, where, among other things, the fields are not at all tightly bound.

Similar reductions in size with traveling wave antennas can be obtained by taking a different approach—modifying the characteristics of the guiding structure itself. The guide wavelength can be expressed in terms of the equivalent circuit parameters of a lossless transmission line as

$$\lambda_g = \frac{1}{\sqrt{LC}}$$

where

L is the series inductance per unit length, and

C is the shunt capacitance per unit length.

By increasing either the series inductance or shunt capacitance (or both) of the line, the guide wavelength can be easily reduced in accordance with the above expression. The series inductance of the slotline in the current spiral antenna is increased dramatically (by a factor of four) by introducing thousands of very narrow, relatively short short-circuited series stubs, as described pictorially in Figure 11 and in more detail in Figure 19. This simple measure reduces the size of the antenna by a factor of two. While more series inductance can be synthesized and added, this served as a very successful feasibility study.

Other miniaturization techniques, such as the addition of lumped element shunt resistors and the application of high-dielectric constant layers to the aperture will also be examined over the next six months. The series shorted inductive stub loading was performed

first because it appeared to offer the greatest potential for significant size reduction while still being planar, inexpensive, and lightweight.

A.7 Slot Termination

Throughout the published literature, it has been shown that some sort of non-reflecting arm termination is necessary for proper operation of spiral antennas [20]. If left out, poor axial ratio and extreme frequency-dependence in both pattern and input impedance results. The most common terminations for wire or printed spirals involve absorptive cavity loading, lumped series resistors, and the application of resistive paint to the periphery of the antenna. Each of these was integrated and tested in the slot spiral, and none were found to interact sufficiently with the fields in the slots to provide adequate attenuation of the energy reflected from the arm terminations.

A new technique was developed for use with slot spiral antennas that avoids interacting with the traveling wave fields directly. Instead, series and parallel lumped element chip resistors are used to deal directly with the transmission line currents. Balanced matched attenuators are built from these resistors as shown in the schematics in Figure 21. These are then cascaded in series as shown on the right in Figure 20 to form the non-reflecting slot arm termination that is required. Figures 9 and 11 show the location of these terminations in the antenna.

Matched attenuators allow control of both their input and output impedance as well as their attenuation, allowing an optimum termination to be designed. They also can be implemented with very small components in a very small area, making them very compact and extremely frequency independent. This is particularly important at low frequencies, where other termination techniques employing either lumped or distributed elements still must be at least one-quarter of a guide wavelength long. The current slot spiral antenna uses

a cascade of 3 matched attenuators, each matched to within 1% and giving approximately 4 dB of attenuation.

A.8 Transition to Termination

The integration of the cascaded matched attenuator termination mentioned above is straightforward except for the implementation of the series resistors. As mentioned previously, series lumped elements are difficult to implement in slotline because the currents are distributed over the very wide conductors. To overcome this difficulty, a transition from low impedance slotline with very wide conductors to high impedance slotline, or co-planar strip (CPS) line, with very narrow conductors was implemented as shown in Figure 22. The essence of this transition is not, however, the change in impedance—rather, it is the reduction in width of the two conductors, which serves to constrain the currents to a relatively narrow region, and allows a small lumped element to interact with the entire amount of current.

The implementation of this transition in the antenna is problematic, however. The reduction in conductor width discussed above involves either drastic modification of the slot geometry or the opening of extra slits in the ground plane/aperture of the antenna. The latter option was thought to be more sensible and less complex overall, and its basic implementation and integration into an unloaded slot spiral antenna are shown respectively in Figure 23 and 9. Because of the drastic change in the impedance of the slotline, extreme care must be taken to ensure that no reflections that would result in increased axial ratio arise from the transition. A Klopfenstein impedance taper [12] is used to minimize the length of the transition for a given performance specification—in the current unloaded antenna, for a reflection coefficient Γ of 0.01 at 200 MHz, the overall length is 0.67λ, or approximately 34 inches.

A.9 Coplanar Waveguide Termination

The implementation of the transition from slotline to coplanar strip line, as discussed above, results in the opening up of two slits in the antenna ground plane. These slits are very tightly coupled to the rest of the antenna through the reactive near field, and become radiating elements in themselves. Thus, as with the original slotline radiators, in order to avoid both reflections from their ends and resonances, these slits must be terminated as well.

Similar in spirit to the termination used for the slotline/coplanar strip line, a series of matched attenuators is used to prevent reflections from the end of each of the slits. These are shown schematically and pictorially in Figures 21 and 20. After the slotline-to-coplanar strip line termination is accomplished, the two slits are brought closer together to form a coplanar waveguide structure where two matched attenuators are implemented in balanced Π-sections. Each subsection yields approximately 5.25 dB of attenuation. Figures 9 and 11 show the termination regions of the current slot spiral antenna, where both the slotline/coplanar strip line termination and the termination arrangement for the extra slits can be seen.

A.10 Substrate

The slot spiral is etched from a double-sided piece of microwave dielectric substrate, a cut-away cross-section of which is shown in Figure 12. The current spirals are built from 20 mil thick Rogers RO4003 with 1 oz. of electro-deposited copper on each side and a relative dielectric constant of 3.38. This substrate was developed for the personal communications industry, and thus is extremely cost effective while still having very good loss characteristics. Earlier slot spirals where built from thinner substrates, but the 20 mil substrate offers better physical rigidity and durability, and matches well with the 87 mil diameter semi-rigid coaxial line used to connect it to the outside world.

A.11 Reflecting Cavity

Most very broadband spiral antennas incorporate a relatively deep absorbing cavity to force unidirectional radiation by absorbing all the energy that radiates into it. This technique has been developed to the point that it works very well, but at the cost of a reduction in directivity of approximately 3 dB, not to mention whatever near field losses might be induced by placing absorber so close to the antenna [20].

A major advantage of the slot spiral is that this absorbing cavity is unnecessary. The use of slot radiators allows a reflecting plane to be placed very close to the antenna instead, also forcing unidirectional radiation, but with very low losses. An increase in directivity of between 2.25 and 2.75 dB is achieved when a reflecting cavity is added to the slot spiral, implying nearly perfect reflection. This reflecting cavity has also been shown to not dramatically increase the axial ratio of the antenna.

The cavity back is placed as close as possible to the antenna, but not so close as to disturb the transmission line fields in the slots before they radiate. The antenna-cavity assembly is shown in Figure 12. Currently the cavity is approximately $\lambda/75$ deep at the lowest operating frequency, or about 1.5 inches deep for the 18-inch diameter inductively loaded slot spiral, which operates down to 100 MHz. Dielectric loading and other types of slot loading are being investigated as possible ways to further increase the bandwidth of this cavity.

A.12 Dielectric Loading

Dielectric loading is another miniaturization techniques often applied to resonant antennas and circuits where the fields are extremely localized. Although the field structure is considerably different, dielectric loading may offer the potential of up to another factor of two reduction in size for the slot spiral antenna. However, extreme care must be taken to ensure

that this loading is applied without disturbing the operation of the rest of the antenna—in particular, the "infinite balun" structure and the shallow reflecting cavity. One technique for integration of the extra dielectric layer is shown in Figure 24, where the dielectric is placed inside the cavity, but in direct contact with the slots were it will have the most effect. The integration of high dielectric constant loading also requires a complete redesign of the entire antenna to maintain proper matching and good axial ratio performance.

B Slot Spiral Parameter List & Specifications

Following is a list of the various dimensions and parameters used to design and fabricate the inductively loaded 18-inch aperture, unless otherwise noted. See Figures 10, 11, and 12 for a representation of the inductively loaded 18-inch slot spiral.

1. Overall diameter: 19.250 inches.
2. Coaxial-to-Microstrip Line Transition
   - Coaxial Cable: Belden Conformable® Coax, Type RG-405/U, .087" OD, 24 AWG center conductor, TFE teflon dielectric, no jacket.
   - Microstrip Line: 50.0 Ω, 44.7 mils wide.
   - Slit Dimensions: 1.500 inches long × 90.0 mils wide.
   - See Figure 14 for detail drawing.
3. Microstrip Infinite Balun
   - Beginning (at periphery): 50.0 Ω, 44.7 mils wide
   - Ending (at periphery): 67.0 Ω, 26.5 mils wide
   - Klopfenstein taper design parameters:
     - Impedance at beginning: 50.0 Ω
     - Impedance at end: 67.0 Ω
     - Maximum Γ: .02 (-34 dB)
     - Minimum operating frequency: 100 MHz
   - Klopfenstein taper dimensions:
     - Length: 31.713 inches
     - See Figure 15 for actual impedance variation with length along taper/balun.
   - Overall microstrip balun length: 66.769 inches
   - Microstrip balun spiral geometry parameters:

Balun Segment	Spiral Type	Growth Rate (mils/rad)	Number of Turns	Arc Length (in)
1	Archimedean	100.0	1.25	3.247
2	Equiangular	0.110	0.50	2.965
3	Equiangular	0.142	0.50	4.437
4	Equiangular	0.130	1.75	42.710
5	Equiangular	0.182	0.21	10.995
6	Equiangular	0.080	0.05	2.930
7	Equiangular	0.001	0.03	1.775

4. Microstrip-Slot Line Transition

   - Microstrip:
     - Impedance: 67.0 Ω
     - Width: 26.5 mils
     - Extension past slot center: 41.0 mils
     - Via diameter: 18.0 mils
   - Slotline:
     - Impedance: 119.1 Ω
     - Width: 30.0 mils
   - See Figure 18 for detail drawing.

5. Slotline

   - Impedance: 119.1 Ω
   - Width: 30.0 mils
   - Overall length (each arm): 67.456 inches
   - Slotline spiral geometry parameters (each arm):

Balun Segment	Spiral Type	Growth Rate (mils/rad)	Number of Turns	Arc Length (in)
1	Archimedean	100.0	1.00	2.126
2	Equiangular	0.130	3.15	61.122
3	Equiangular	0.050	0.12	6.335

6. Inductive Loading

   - Width of loading slots: 10 mils
   - Loading slot center-to-center distance: 20 mils
   - Length: Determined by linear interpolation from shorted to longest stub. Longest stub length is one-third the separation between slots at its location.
     - Shortest stub: 0.5 mils
     - Longest stub: 906 mils
   - Start Diameter: $\approx$ 1.875 inches
   - Number of Stubs: 5560 per slot arm
   - See Figure 19 for detail view.

7. Slot Termination

   - Matched attenuators; balanced T-section:
     - System impedance: 131.5 Ω
     - Strip width: 125 mils
     - Slot width: 30 mils
     - Attenuation per section: 4.05 dB
     - Number of sections: 3
     - Total attenuation: 12.15 dB
     - Series resistor (× 4):
       * Resistance: 15 Ω
       * Specifications: 1 Watt, 5%, case 2512
     - Parallel resistor:
       * Resistance: 274 Ω
       * Specifications: 1/16 Watt, 1%, case 0603
     - Section length: 1.034 inches
     - Overall length: 3.102 inches
     - See Figures 20 and 21 for detail views.

8. Transition to Termination (for unloaded 18-inch aperture only)

   - Scaled Klopfenstein impedance taper, design parameters:
     - Impedance at beginning: 50 Ω
     - Impedance at end: 100 Ω
     - Maximum Γ: .01 (-40 dB)
     - Minimum operating frequency: 200 MHz
   - Scaled Klopfenstein impedance taper dimensions:
     - Length: 18.644 inches

9. Coplanar Waveguide Termination

   - Matched attenuators; balanced Π-section:
     - System impedance: 160.0 Ω
     - Strip width: 100 mils
     - Slot width: 200 mils
     - Section length: 1.034 inches
     - Attenuation per section: 5.25 dB
     - Number of sections: 2
     - Total attenuation: 10.5 dB
     - Series resistor:
       * Resistance: 100 Ω
       * Specifications: 1/2 Watt, 5%, case 2010
     - Parallel resistor ($\times$ 4):
       * Resistance: 1100 Ω
       * Specifications: 1 Watt, 5%, case 2512
     - Section length: 949 mils
     - Overall length: 1.898 inches
     - See Figures 20 and 21 for detail views.

10. Substrate

    - Rogers RO4003® Series glass reinforced hydrocarbon/ceramic laminate:
      - Thickness: 20 mils
      - Cladding: 1 oz / 1 oz electrodeposited copper
      - Relative dielectric constant @ 10 GHz: $\epsilon_r = 3.38 \pm 0.05$
      - Dissipation factor @ 10 GHz: .0027
      - Standard FR-4 processing

11. Reflecting Cavity

    - Depth: 500 mils
    - Diameter: 18.250 inches

C Patterns

Frequency	SPI8.2	SPI9.2
100 MHz	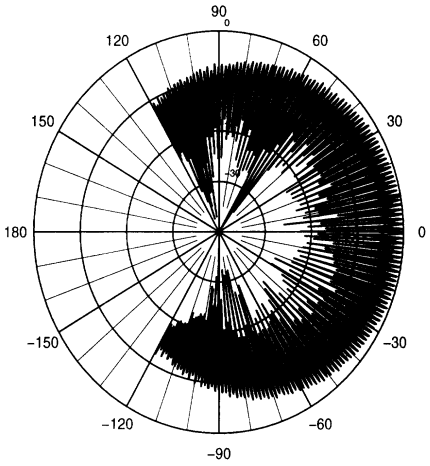	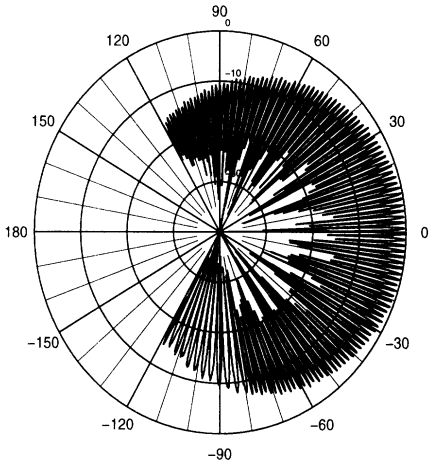
150 MHz	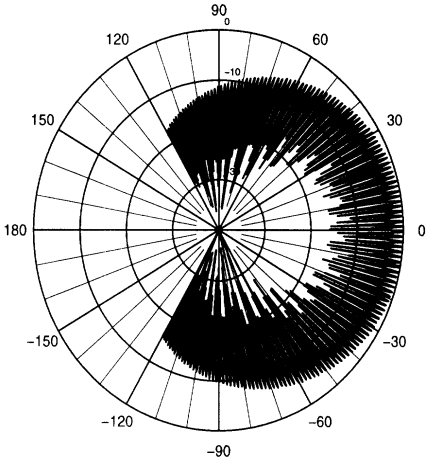	(Not Measured)
200 MHz	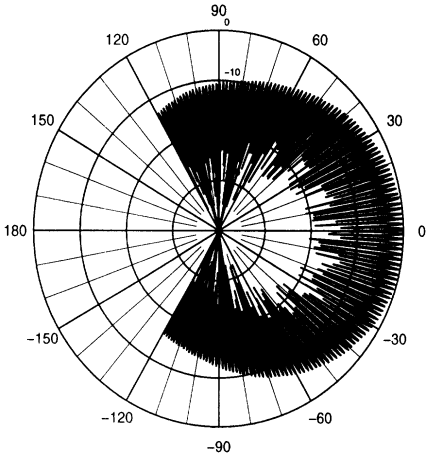	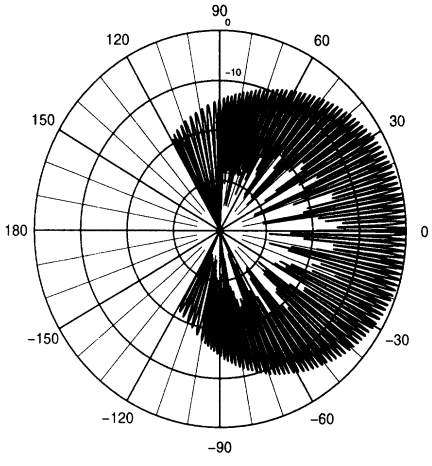

Frequency	SPI8.2	SPI9.2
300 MHz	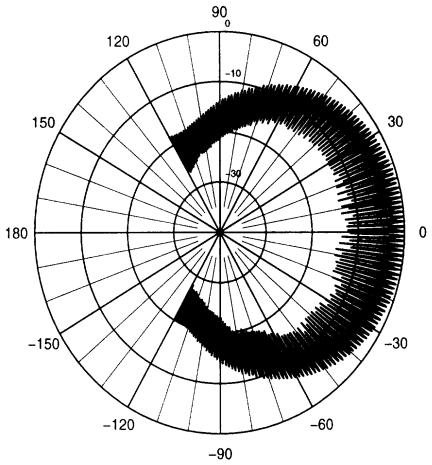	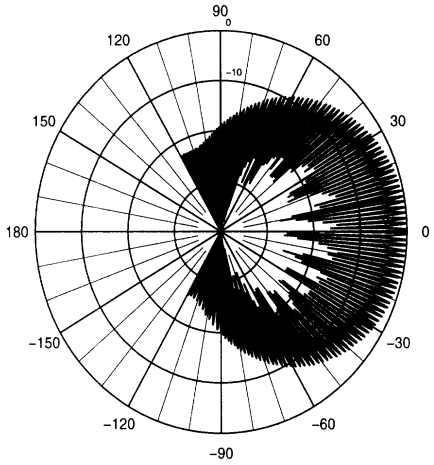
400 MHz	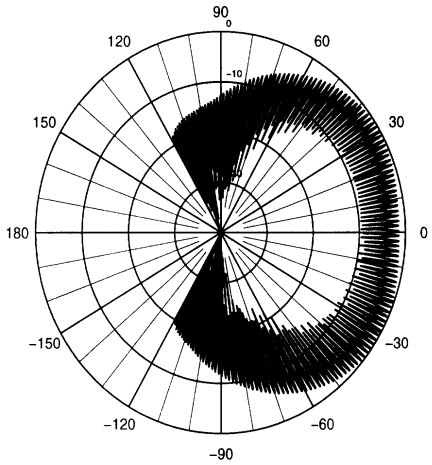	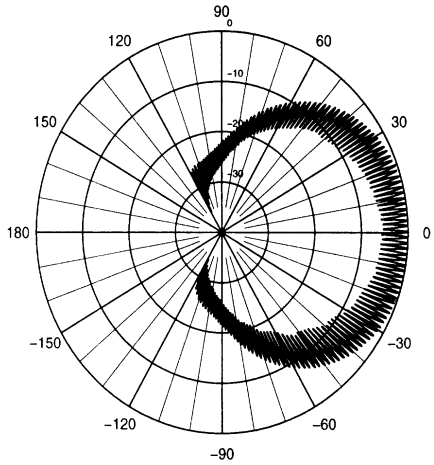
500 MHz	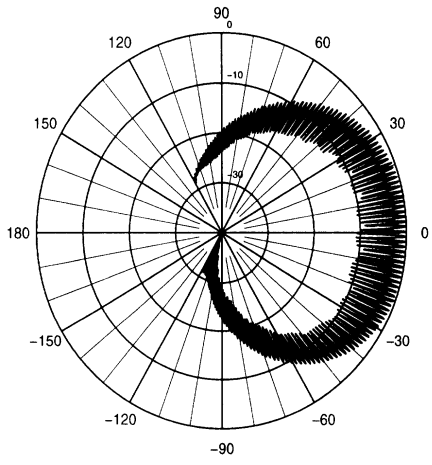	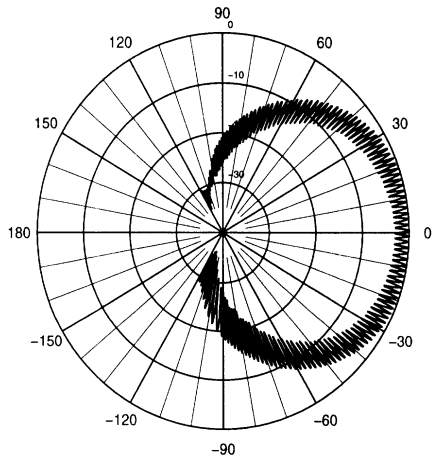

Frequency	SPI8.2	SPI9.2
600 MHz	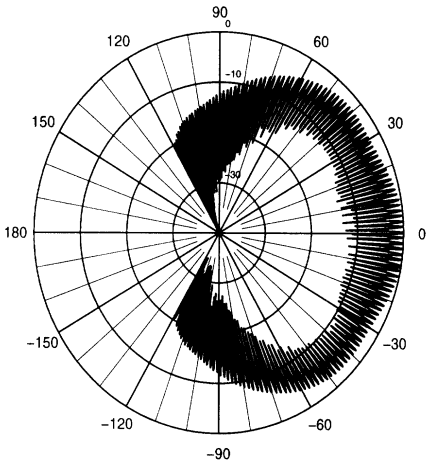	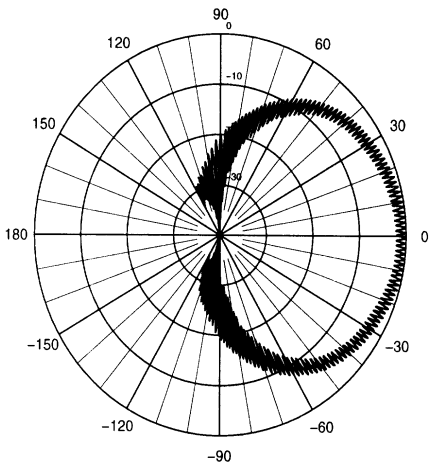
700 MHz	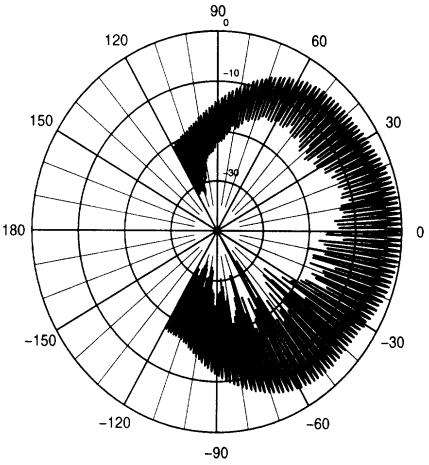	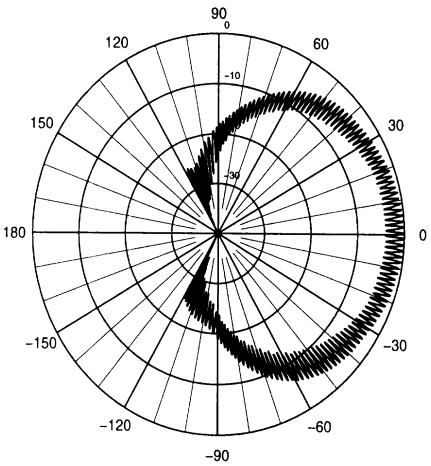
800 MHz	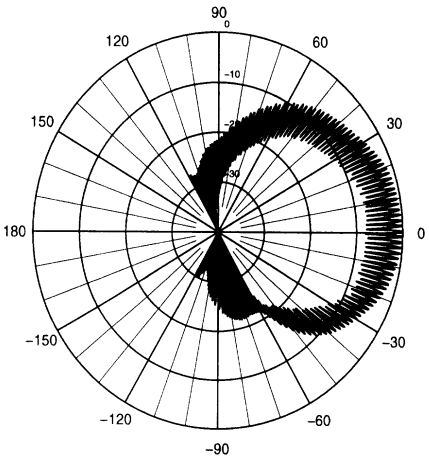	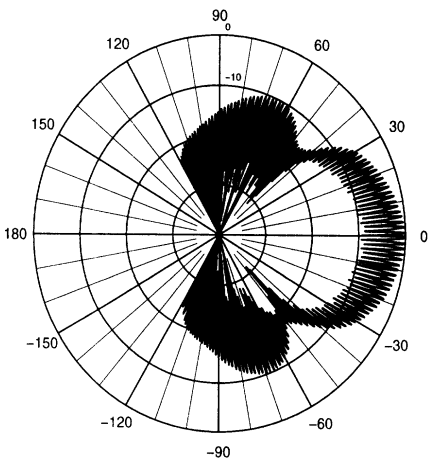

Frequency	SPI8.2	SPI9.2
900 MHz	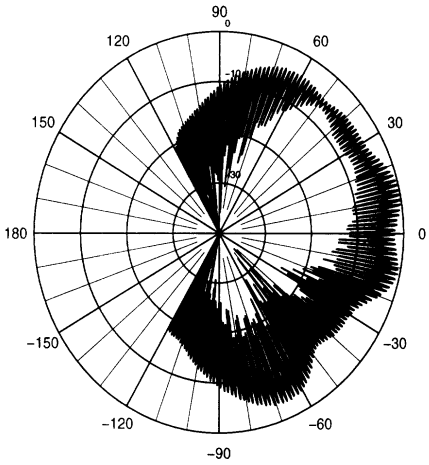	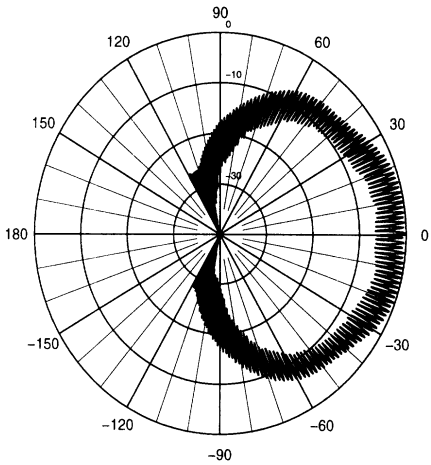
1000 MHz	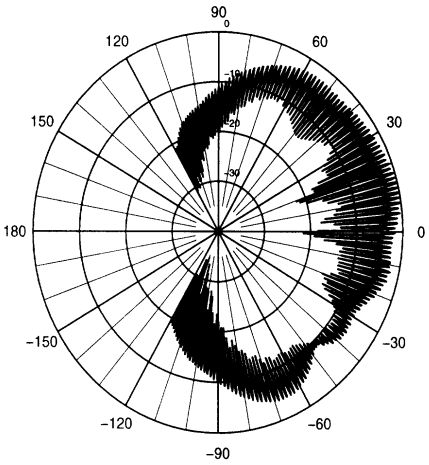	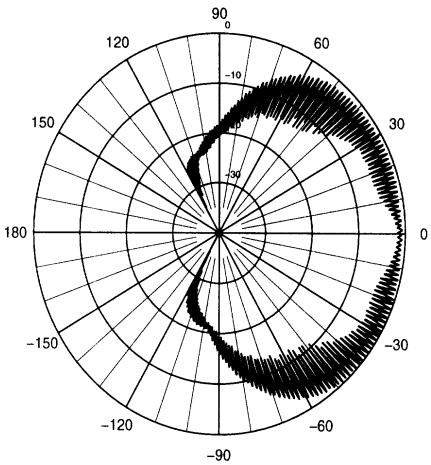
1100 MHz	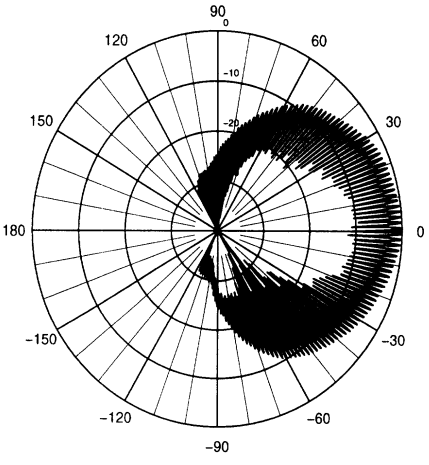	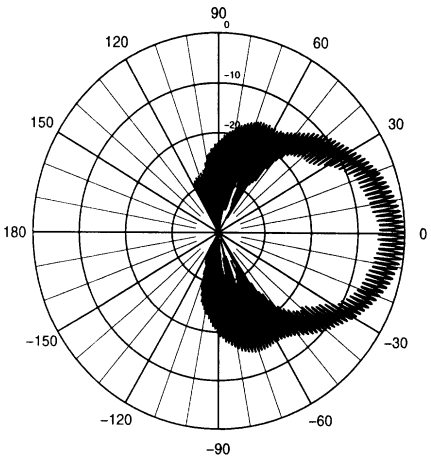

Frequency	SPI8.2	SPI9.2
1200 MHz	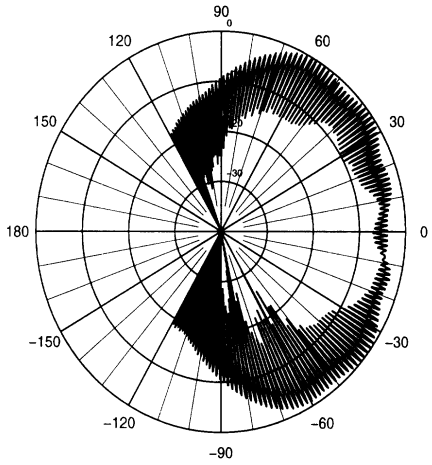	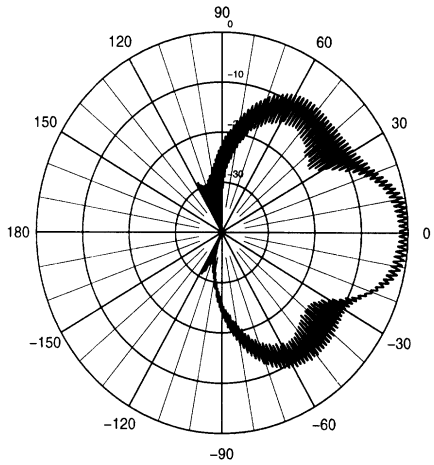
1300 MHz	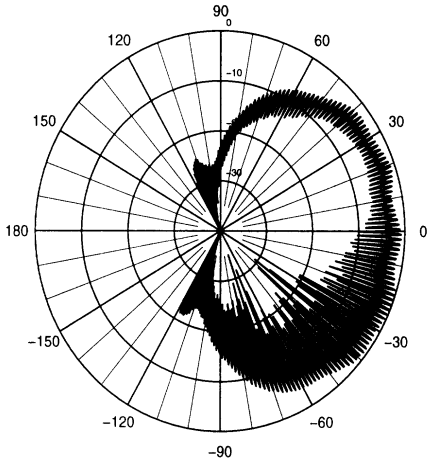	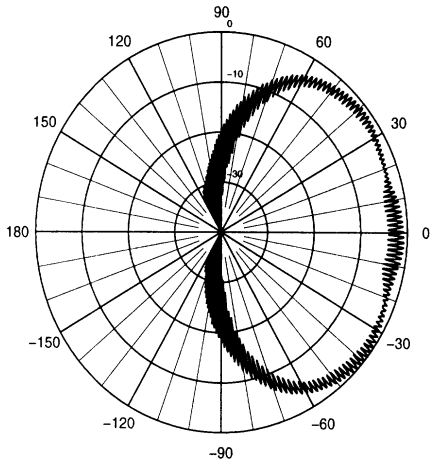
1400 MHz	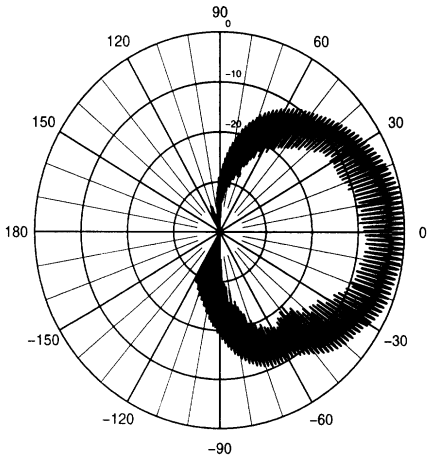	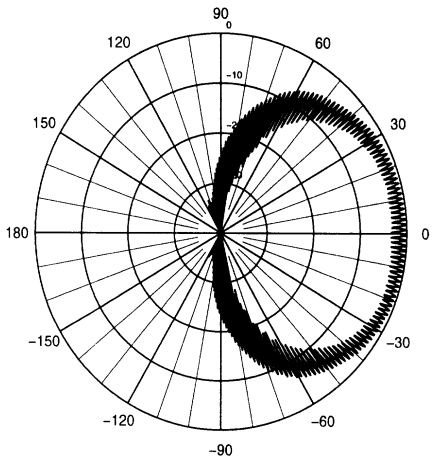

Frequency	SPI8.2	SPI9.2
1500 MHz	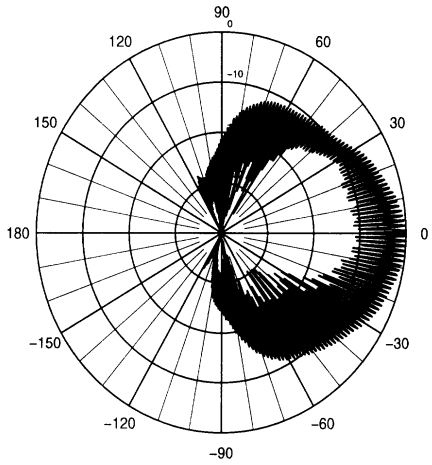	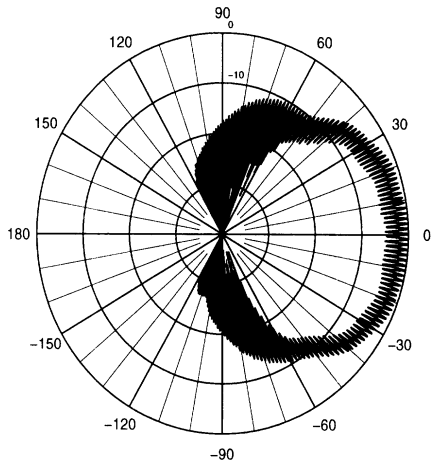
1600 MHz	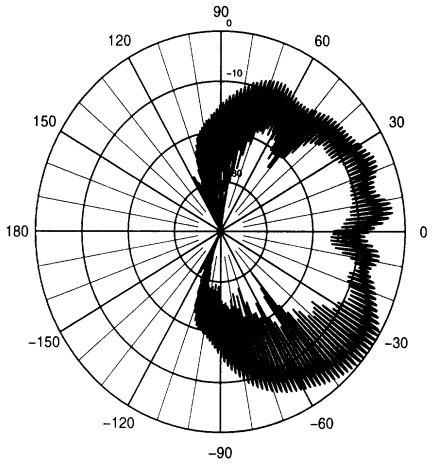	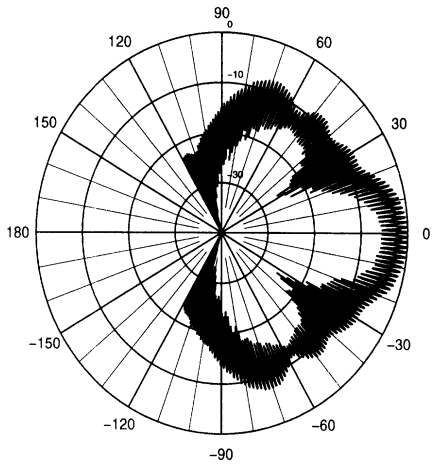
1700 MHz	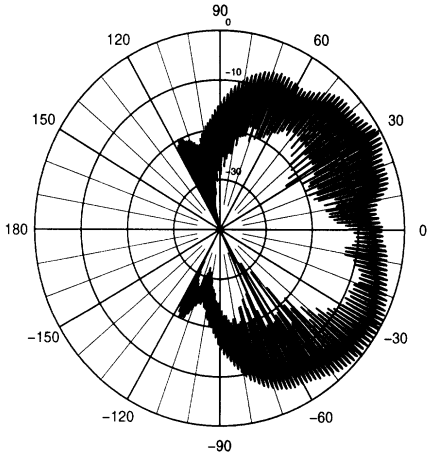	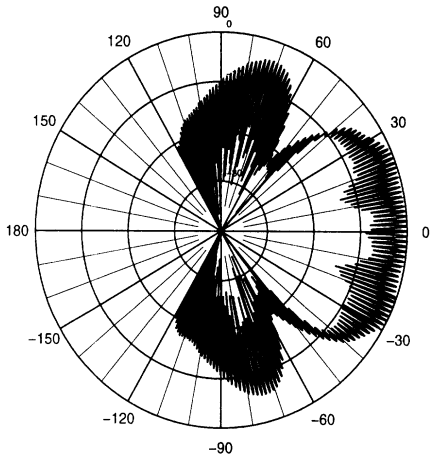

Frequency	SPI8.2	SPI9.2
1800 MHz	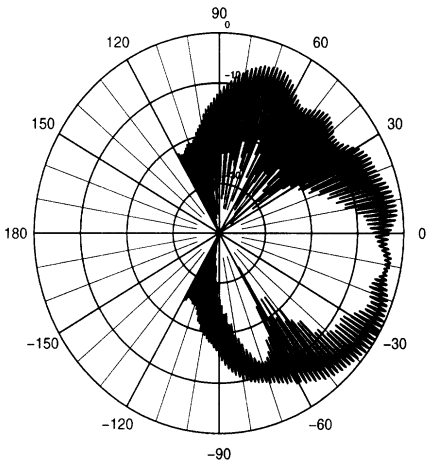	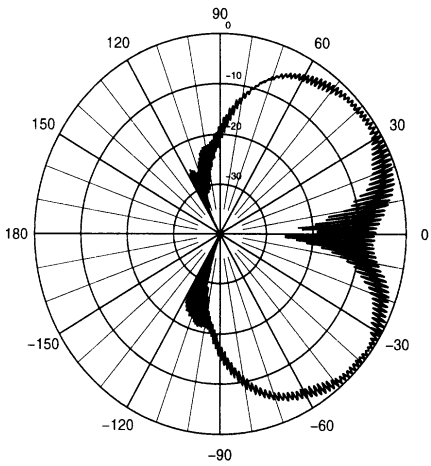
1900 MHz	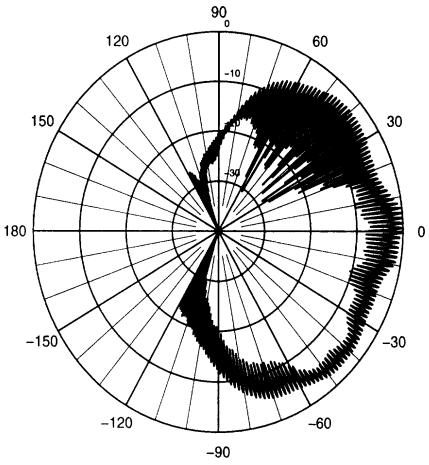	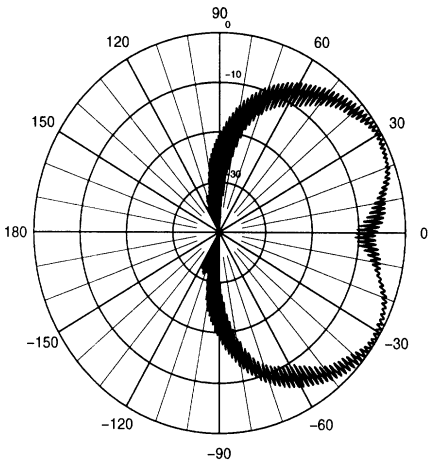
2000 MHz	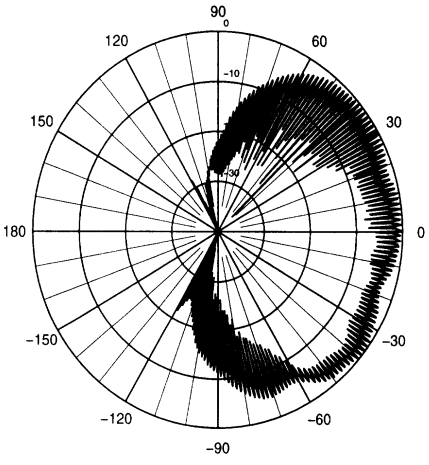	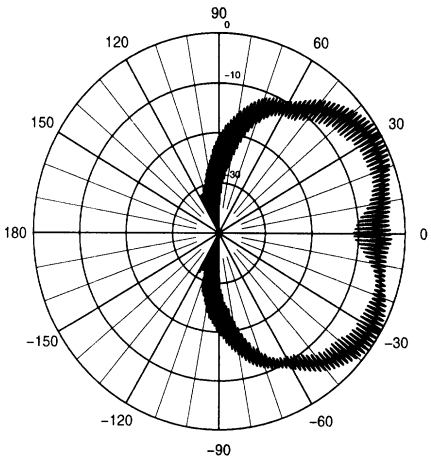

Frequency	SPI8.2	SPI9.2
2100 MHz	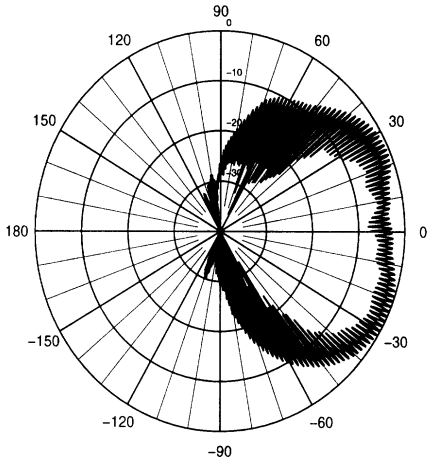	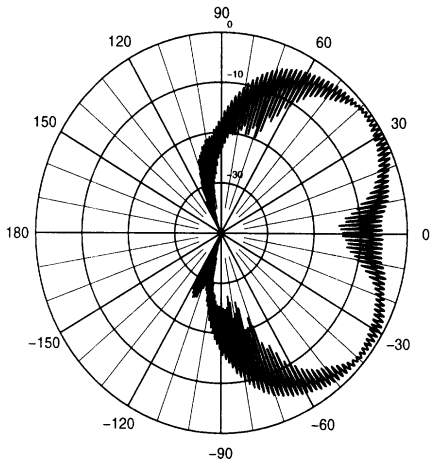
2200 MHz	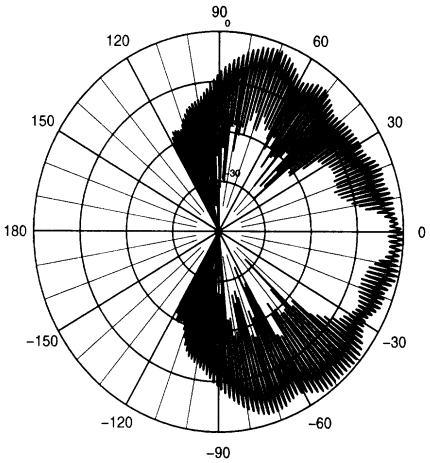	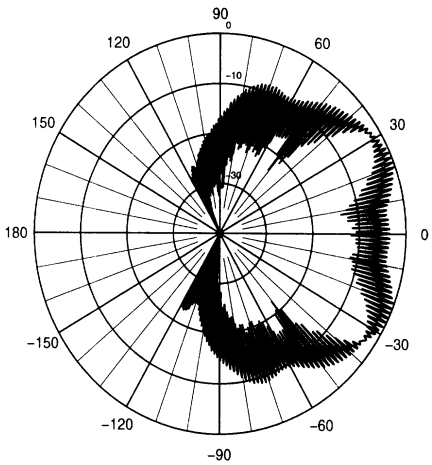
2300 MHz	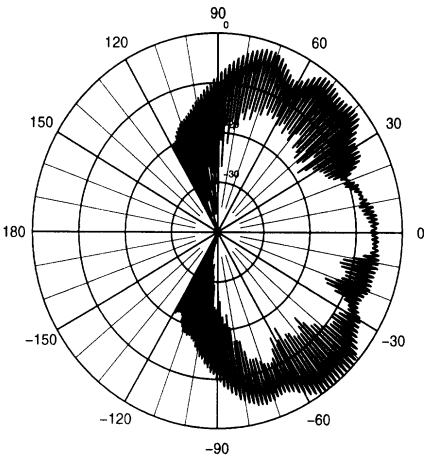	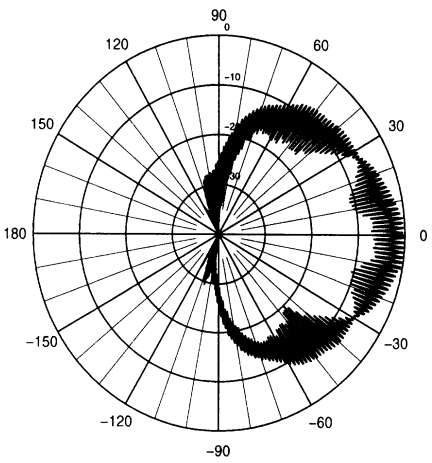

Frequency	SPI8.2	SPI9.2
2400 MHz	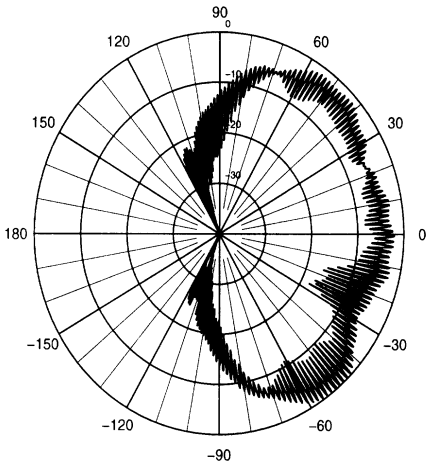	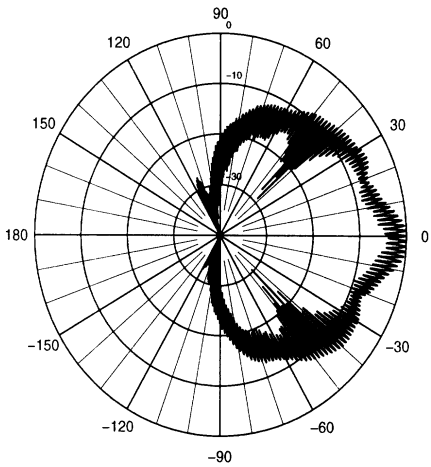
2500 MHz	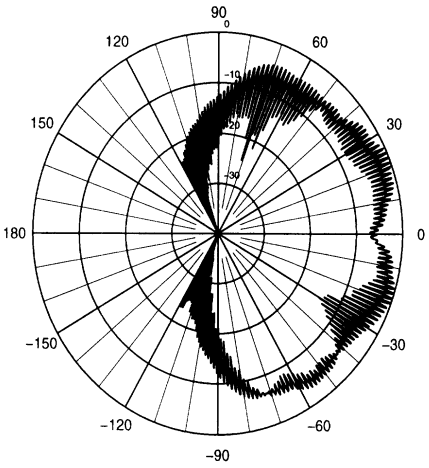	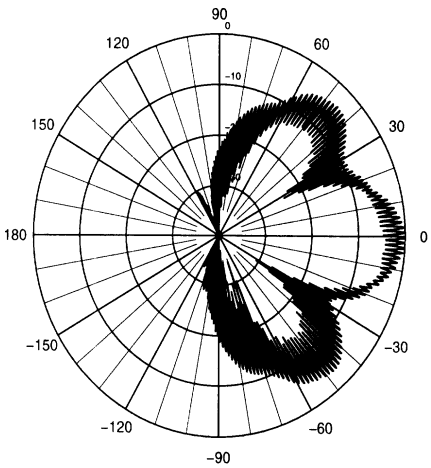
2750 MHz	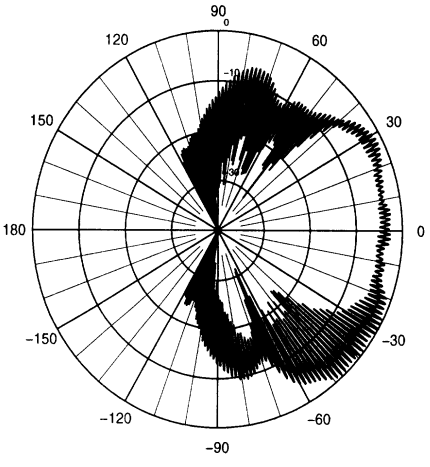	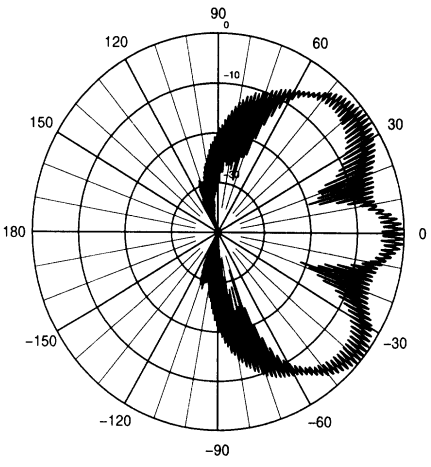

Frequency	SPI8.2	SPI9.2
3000 MHz	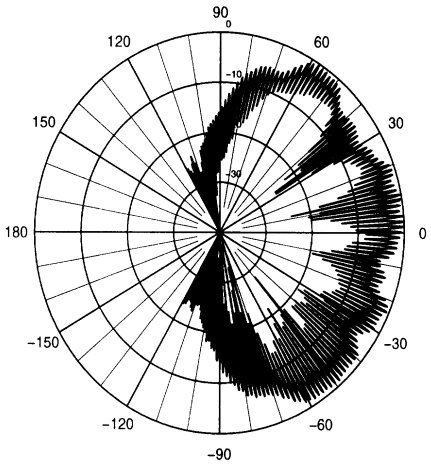	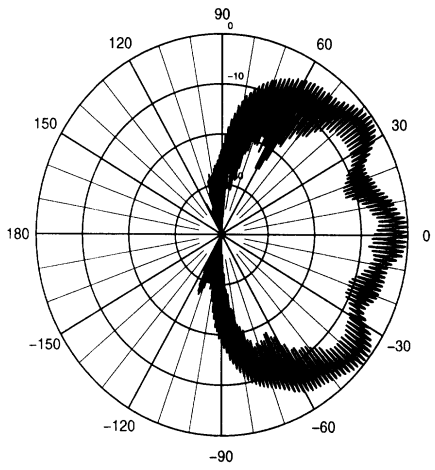

D Figures

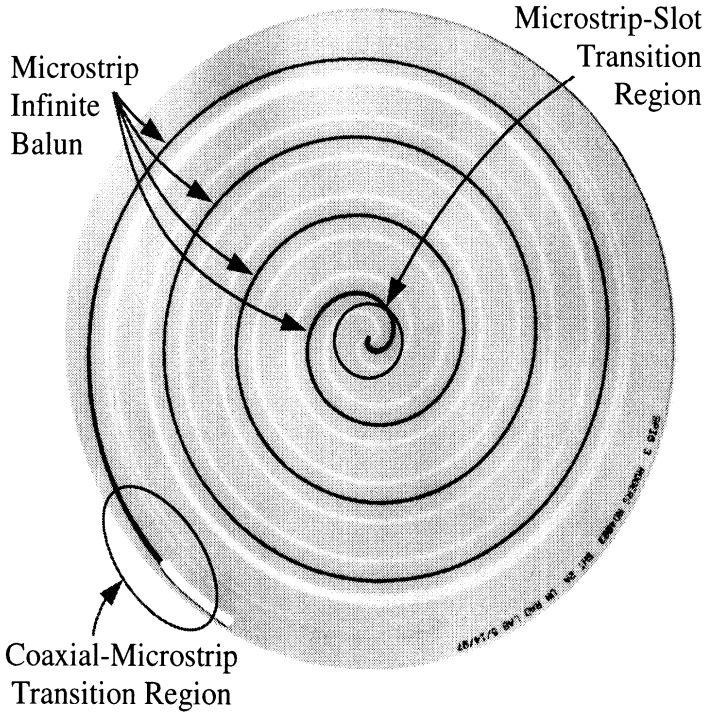

Figure 1: Front (Top) of Previous State-of-the Art 6" Slot Spiral.

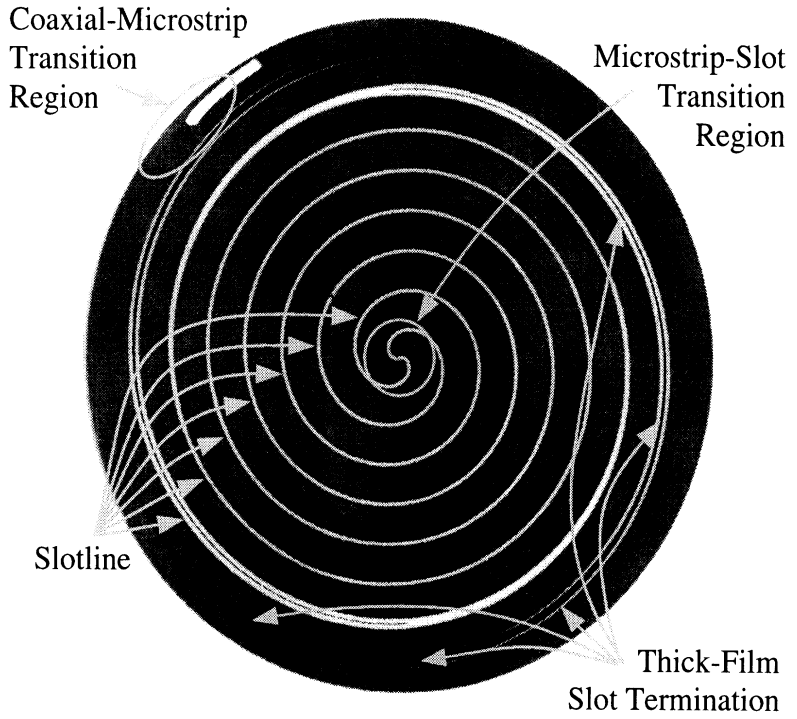

Figure 2: Back (Bottom) of Previous State-of-the Art 6" Slot Spiral.

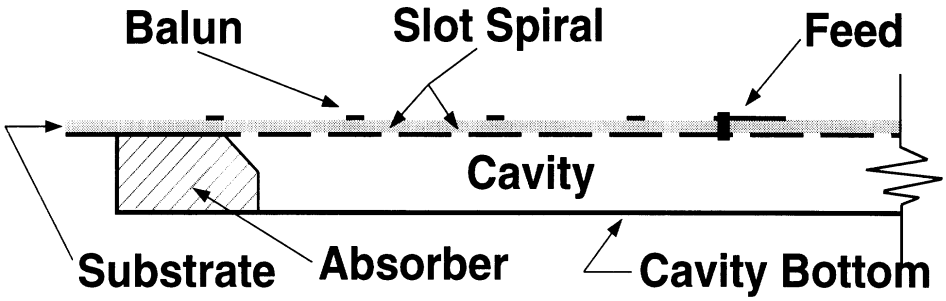

Figure 3: Cross-Section of Reflecting Cavity for Previous State-of-the-Art 6" Slot Spiral.

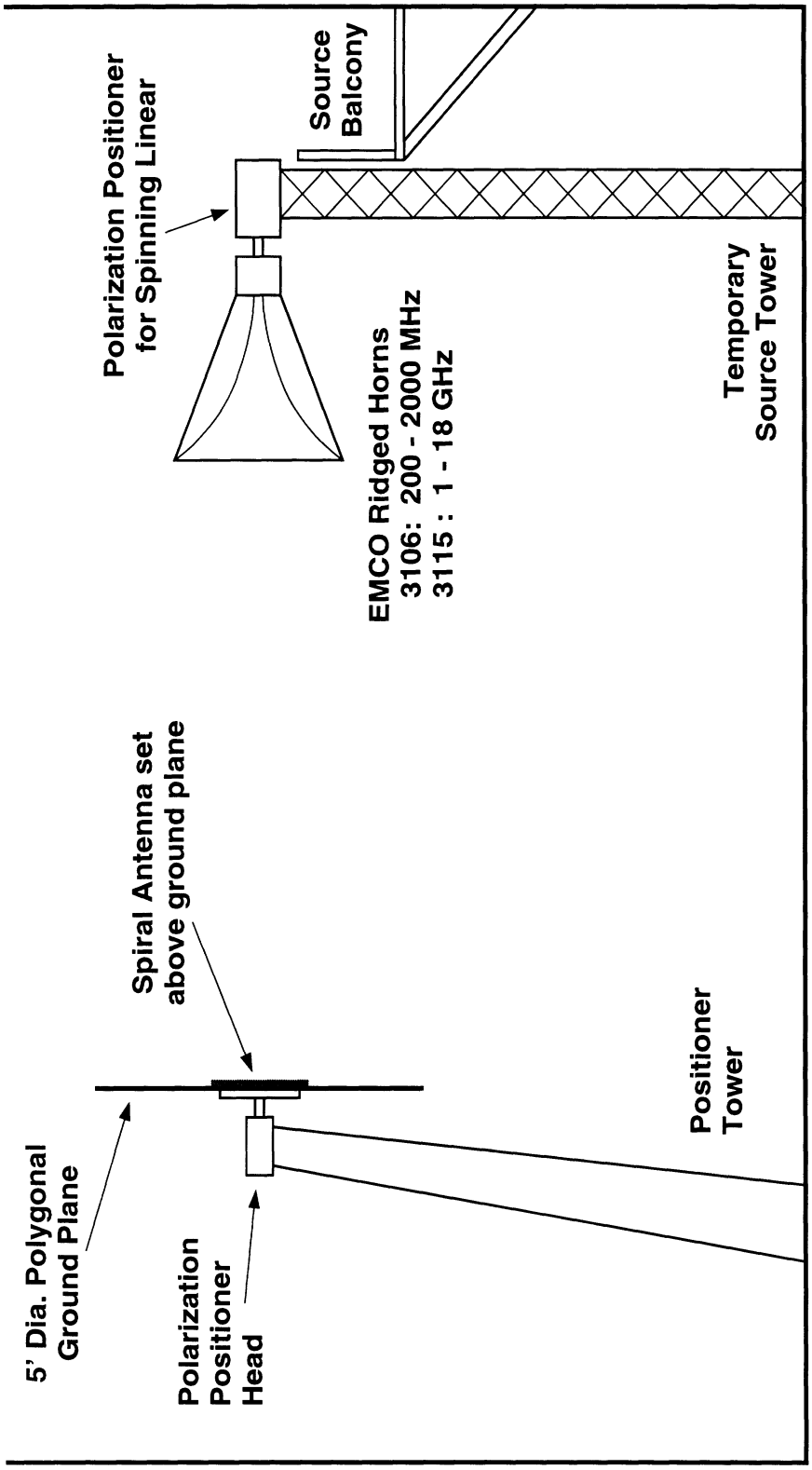

Figure 4: Schematic of Measurement Setup in Anechoic Chamber at Rome Laboratories.

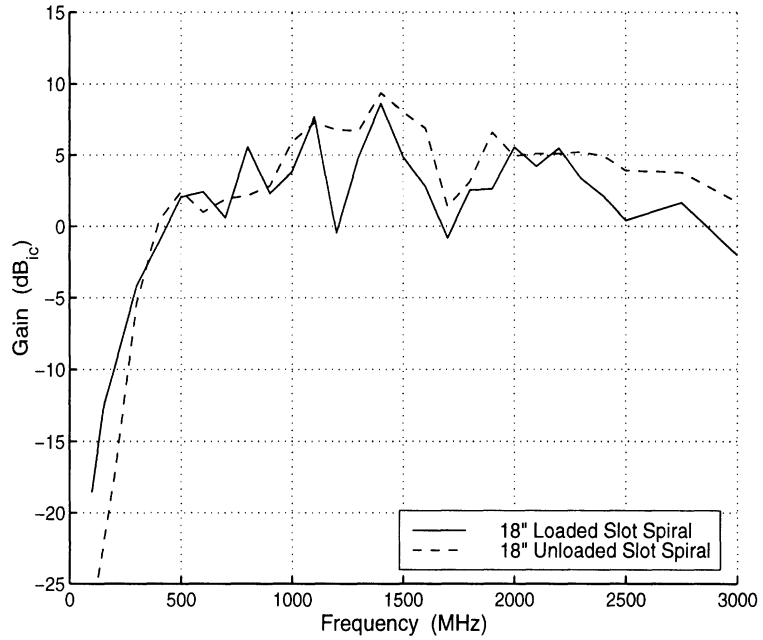

Figure 5: Boresight Gain of Loaded and Unloaded 18-inch Diameter Slot Spiral Antennas (SPI9 and SPI8, Respectively).

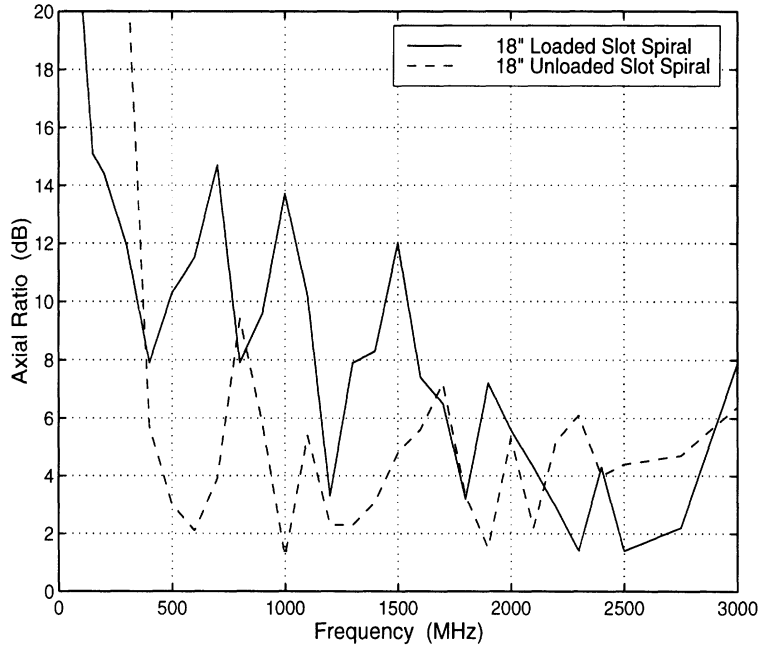

Figure 6: Boresight Axial Ratio of Loaded and Unloaded 18-inch Diameter Slot Spiral Antennas (SPI9 and SPI8, Respectively).

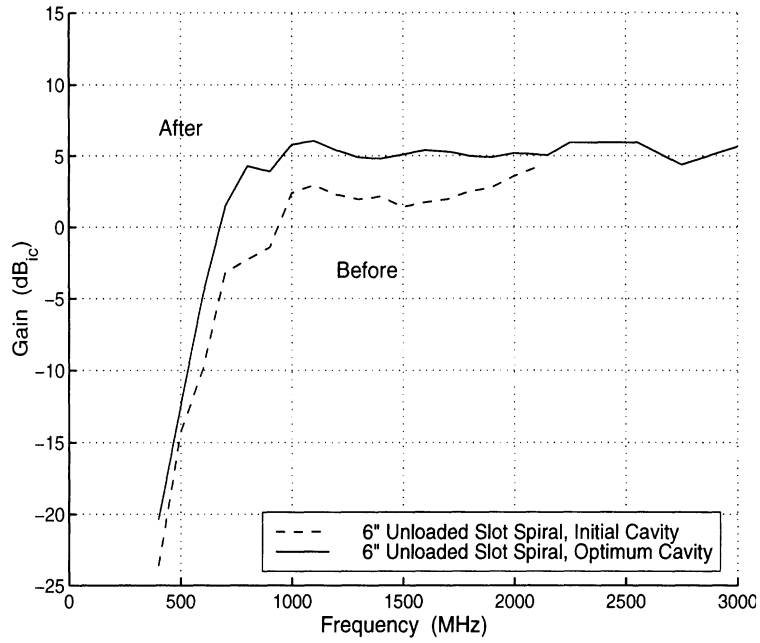

Figure 7: Resulting Improvement in Gain by Doubling Cavity Depth in Previous State-of-the-Art Slot Spiral Antenna.

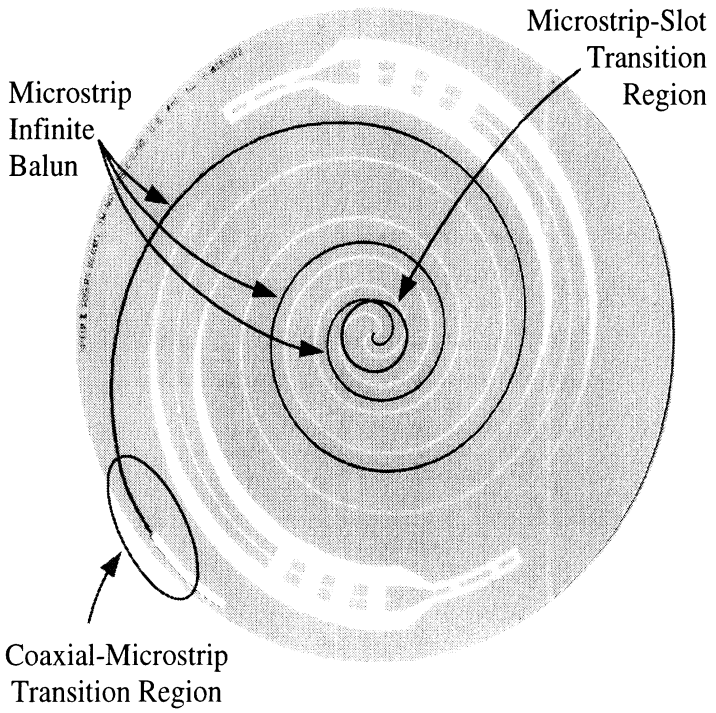

Figure 8: Front (Top) of SPI10 - Unloaded Version of Current Slot Spiral.

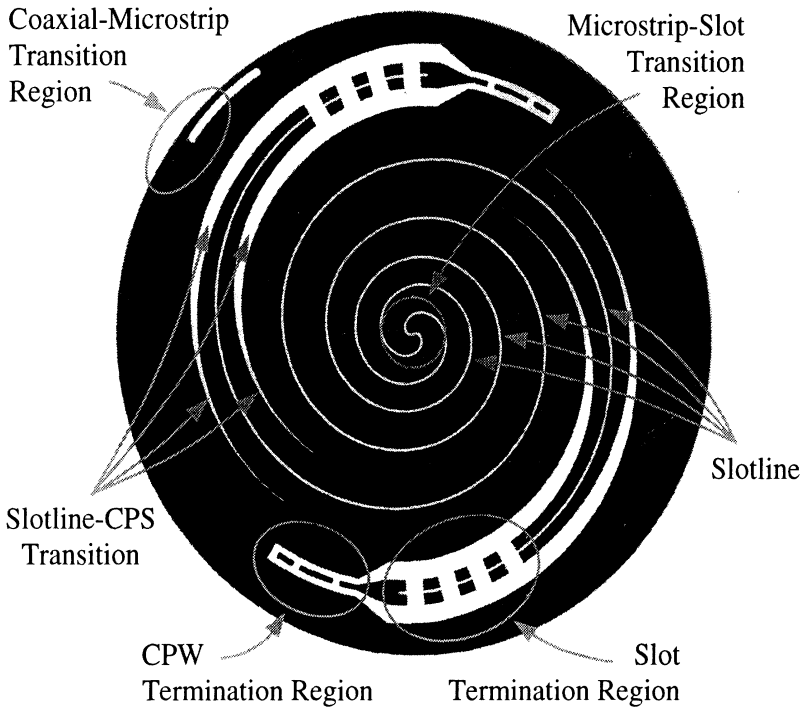

Figure 9: Back (Bottom) of SPI10 - Unloaded Version of Current Slot Spiral.

NOTE: These are the 6" dia. equivalents of SPI9, the 18" dia. unloaded spiral.

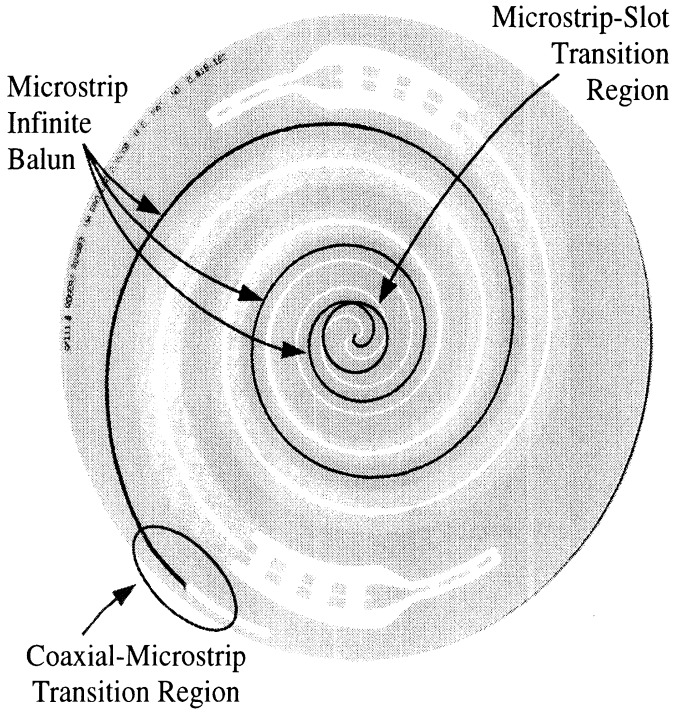

Figure 10: Front (Top) of SPI11 - Inductively Loaded Version of Current Slot Spiral.

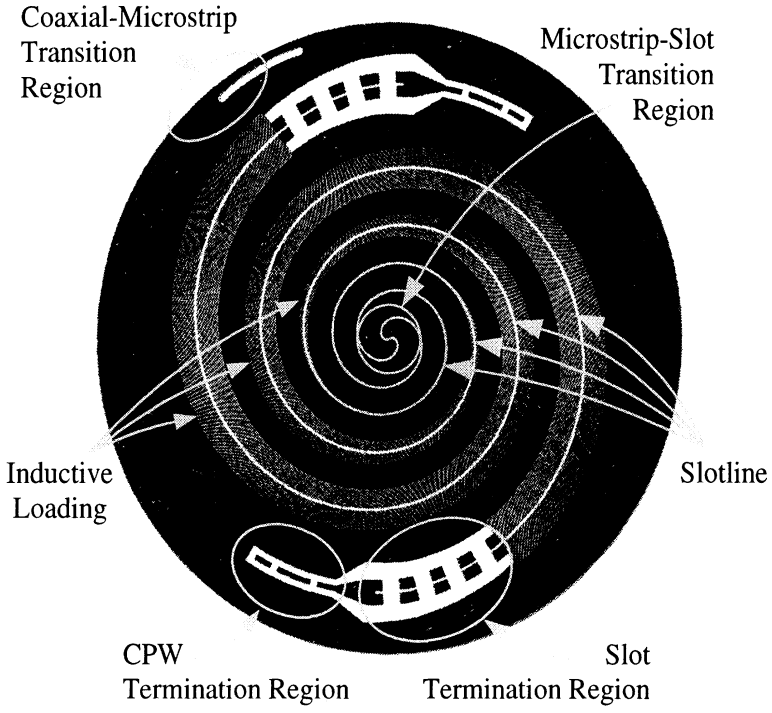

Figure 11: Back (Bottom) of SPI11 - Inductively Loaded Version of Current Slot Spiral.

NOTE: These are the 6" dia. equivalents of SPI8, the 18" dia. loaded spiral.

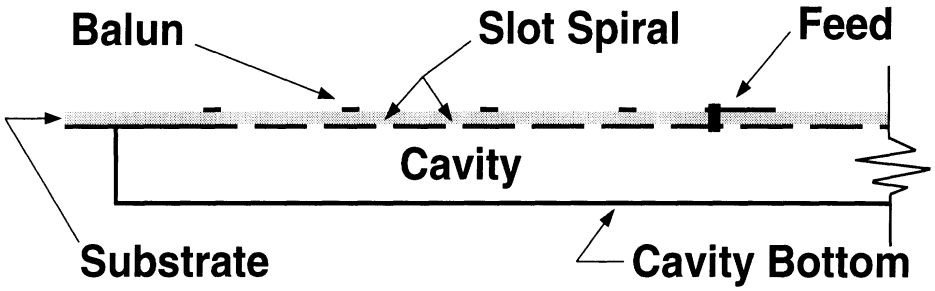

Figure 12: Cross-Section of Typical Slot Spiral with Reflecting Cavity.

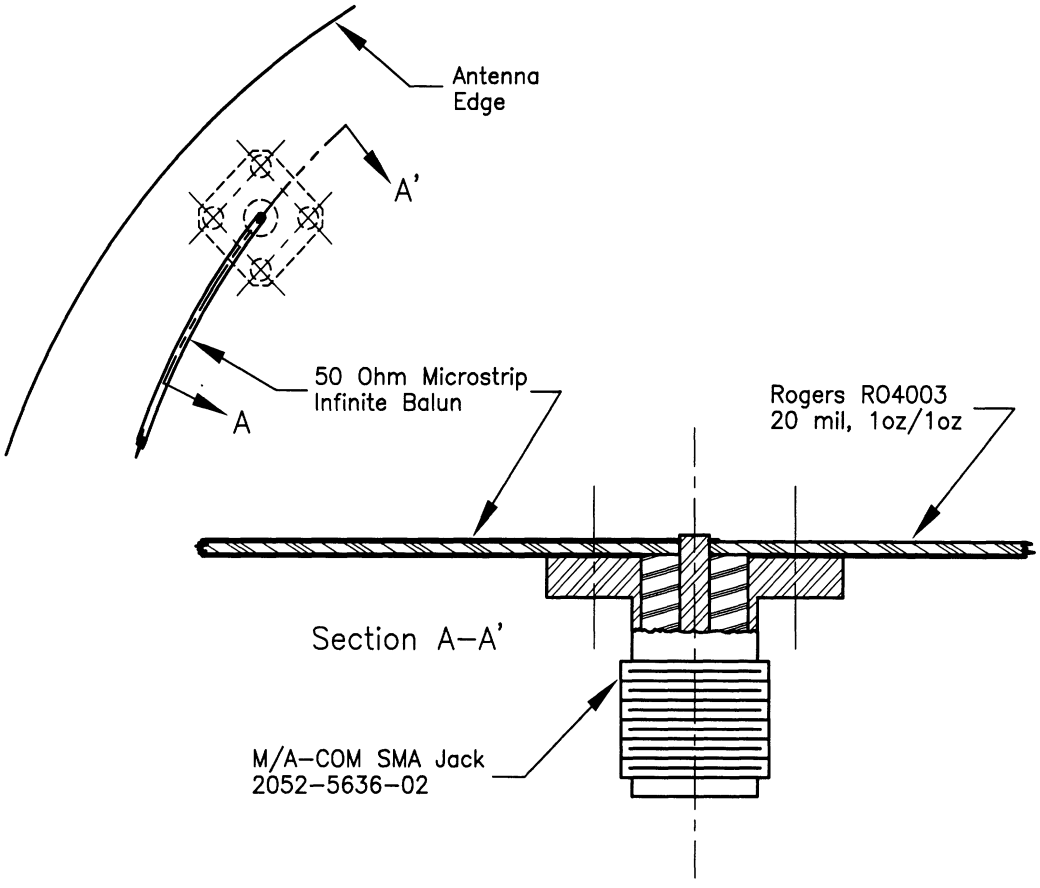

Figure 13: Right-angle transition from Coaxial Cable/SMA Connector to Microstrip Line.

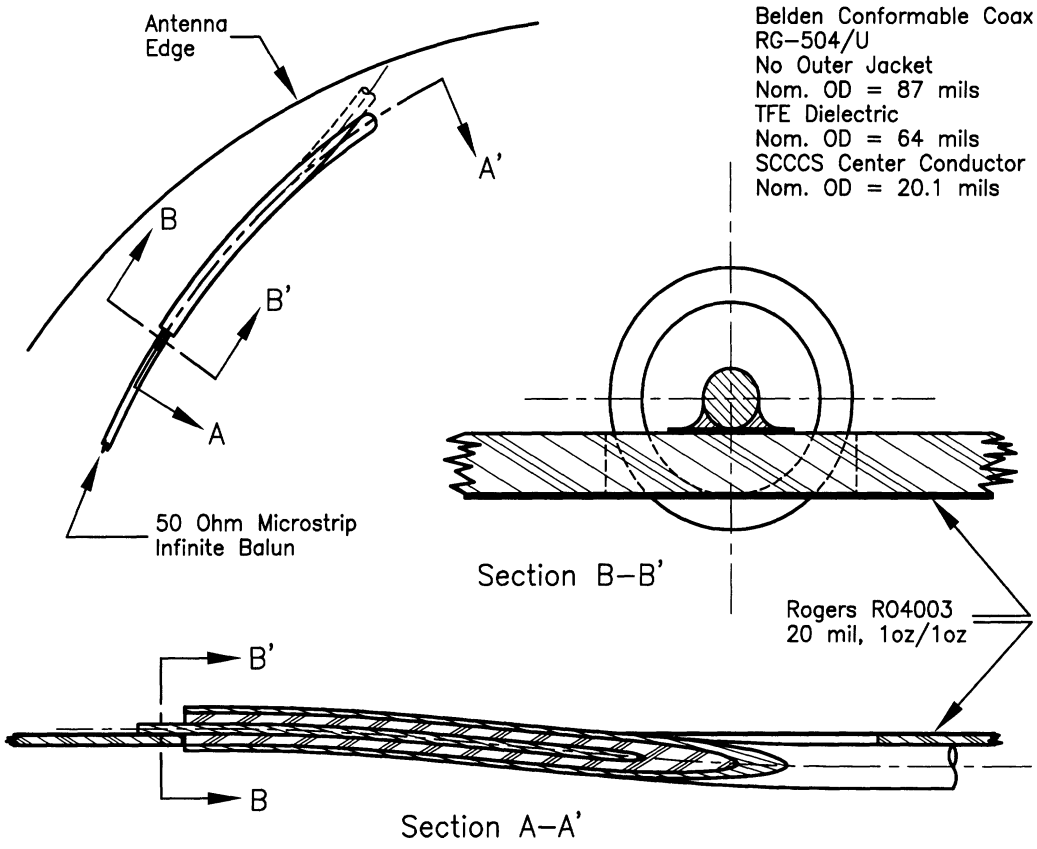

Figure 14: Inline Transition from Coaxial Cable to Microstrip Line.

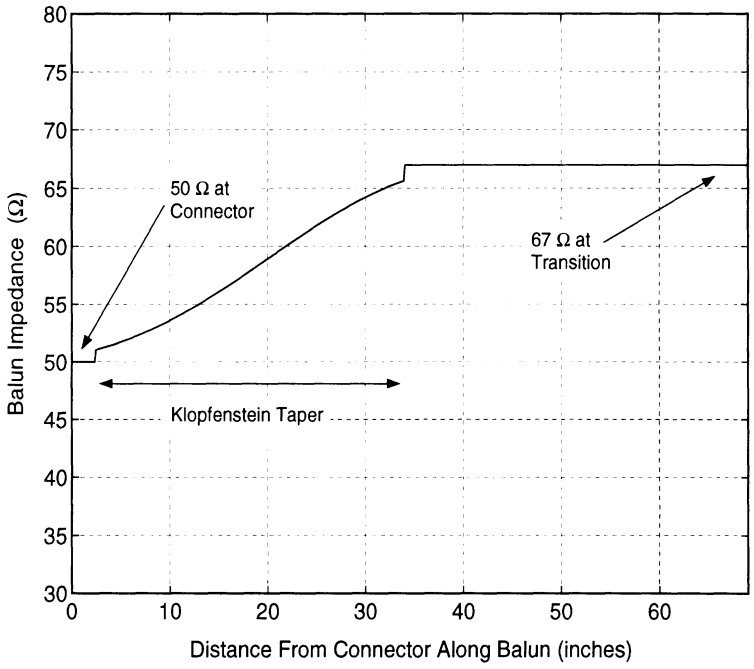

Figure 15: Impedance Variation Along Microstrip Infinite Balun, from the Coaxial-to-Microstrip Transition (0.000") to the Microstrip-to-Slotline Transition (69.019").

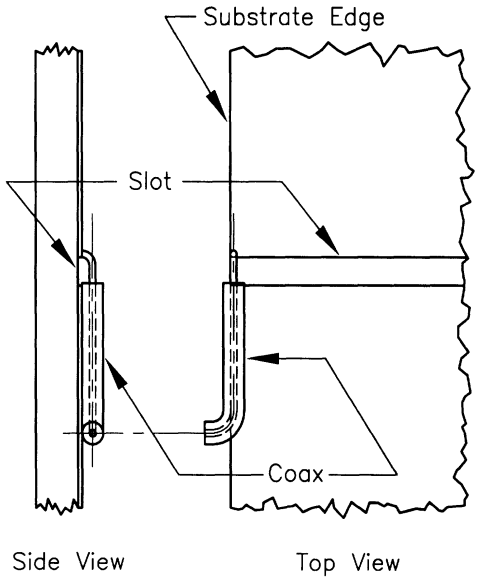

Figure 16: Transition from Coaxial Line to Slotline.

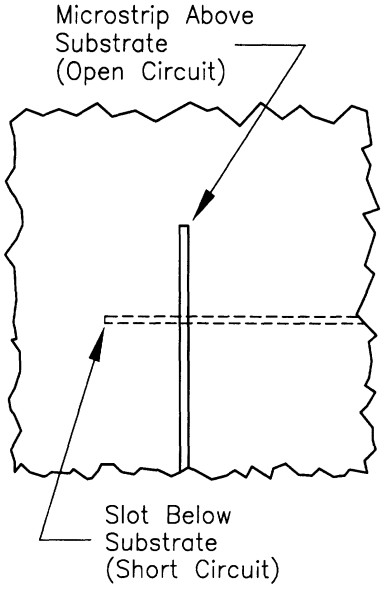

Figure 17: Transition from Microstrip Line to Slotline.

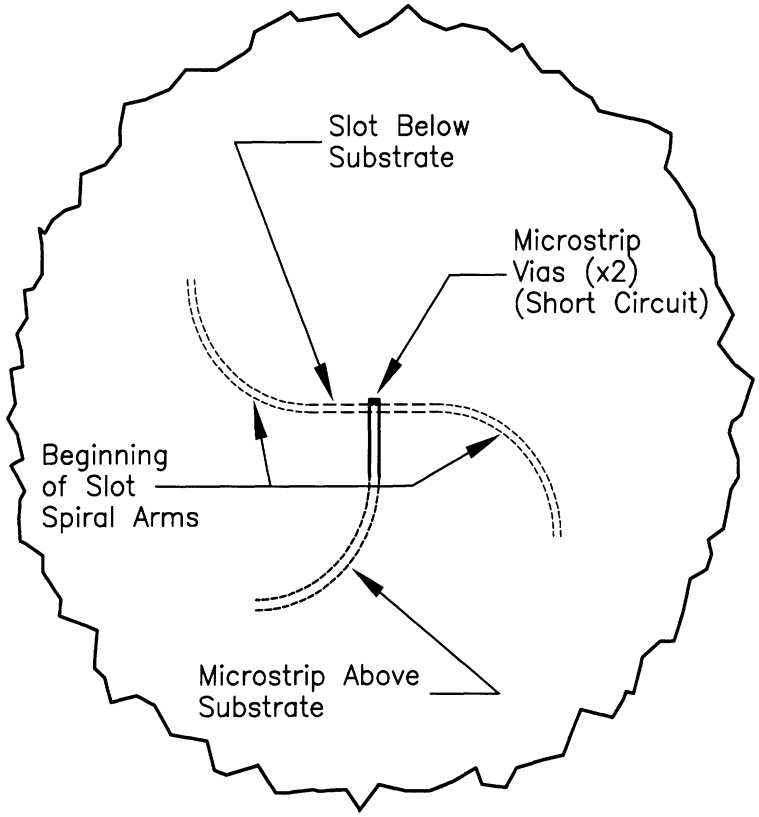

Figure 18: Symmetric Version of Microstrip-to-Slotline Transition.

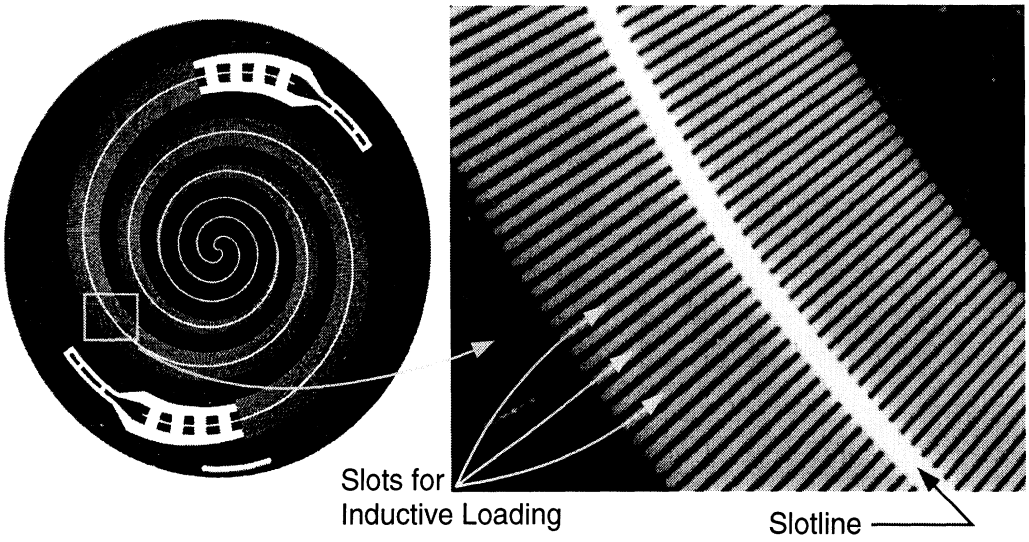

Figure 19: Detail View of Inductively-Loaded Slotline. Shows the Individual Short, Narrow Short-Circuit Slots on Each Side of the Main Sotline.

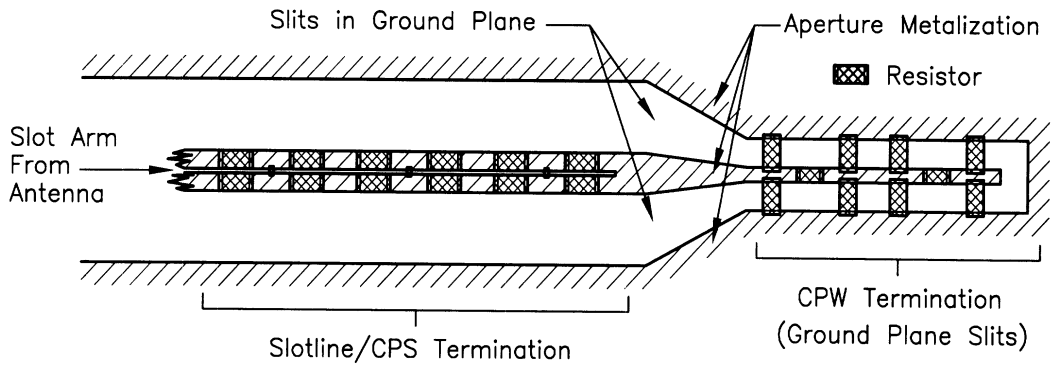

Figure 20: Slot/CPS Termination and CPW Termination as Implemented in the Antenna.

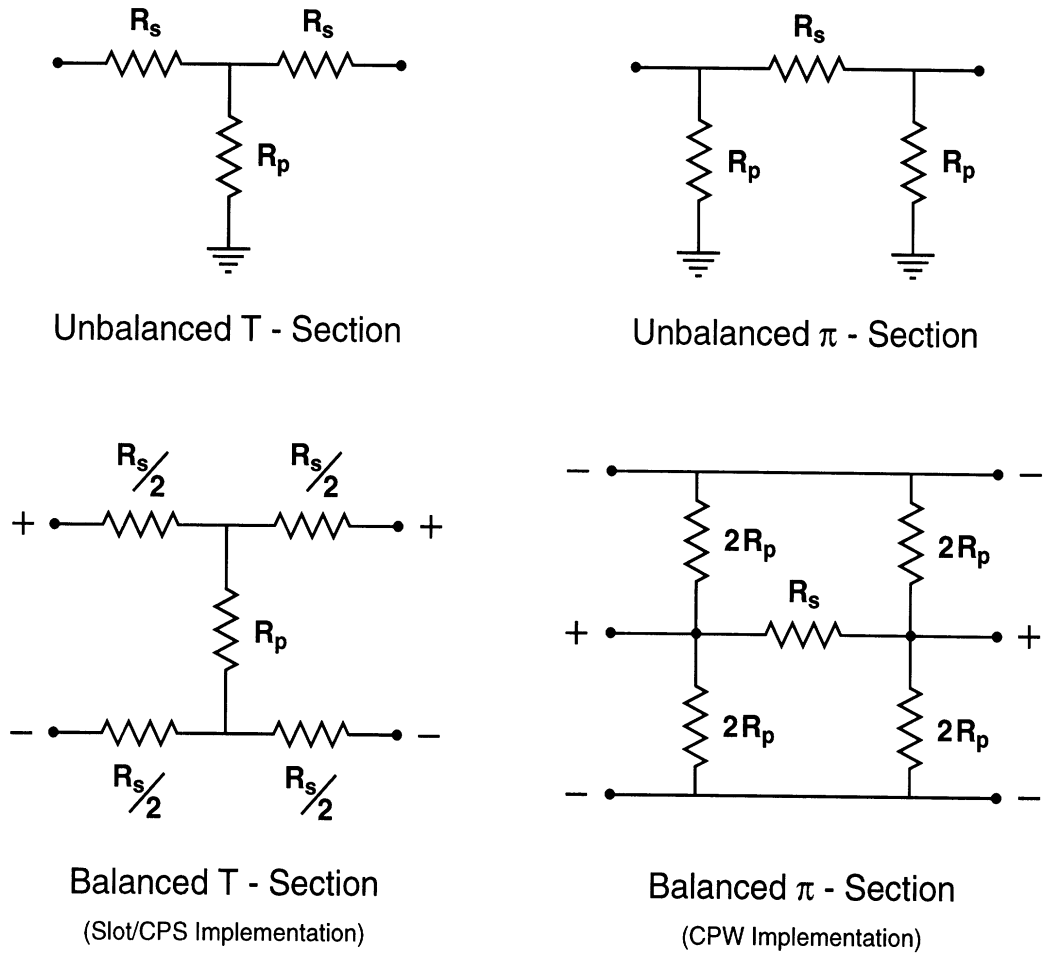

Figure 21: Matched Attenuator Realizations. Typical Unbalanced Implementations Shown at Top; Balanced Implementation Used In Termination of Spiral Antenna Shown at Bottom.

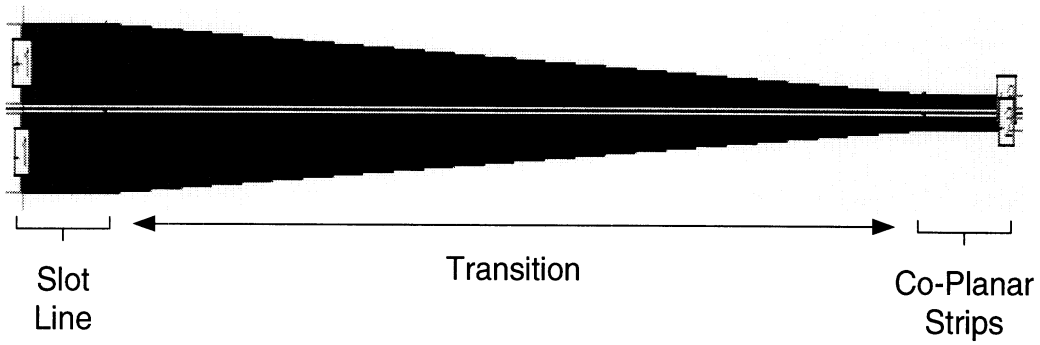

Figure 22: Transition from Slotline to Co-Planar Strips Showing Dramatic Decrease in Conductor Widths.

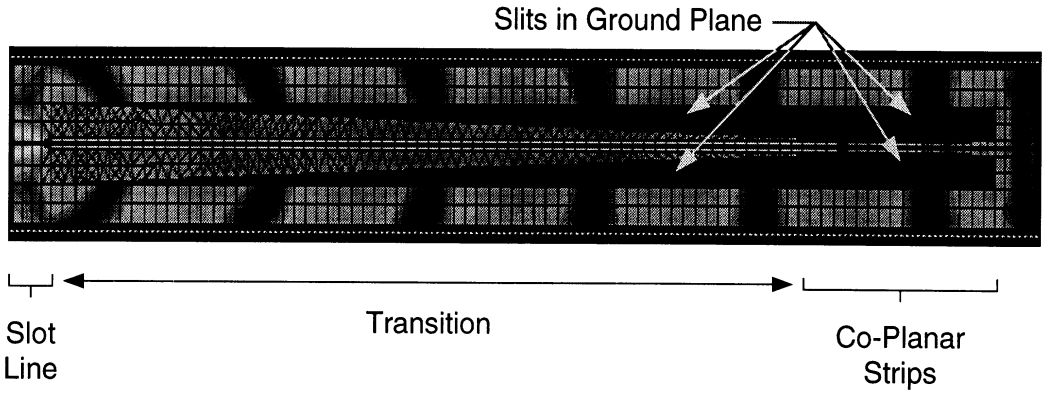

Figure 23: Transition from Slotline to Co-Planar Strips Showing Necessary Openings in Conducting Plane of the Antenna.

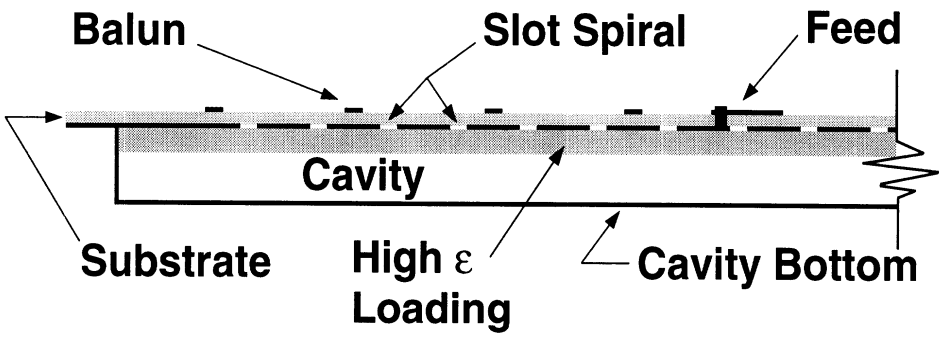

Figure 24: Cross-section of dielectric-loaded spiral and cavity showing placement of dielectric layer in caviy.